

Article

Proteomic Comparison of Acute Myeloid Leukemia Cells and Normal CD34⁺ Bone Marrow Cells: Studies of Leukemia Cell Differentiation and Regulation of Iron Metabolism/Ferroptosis

Frode Selheim¹, Elise Aasebø², Håkon Reikvam^{2,3} , Øystein Bruserud^{2,3,*} and Maria Hernandez-Valladares^{1,4,5}

¹ Proteomics Unit of University of Bergen (PROBE), University of Bergen, Jonas Lies vei 91, 5009 Bergen, Norway; frode.selheim@uib.no (F.S.); mariahv@ugr.es (M.H.-V.)

² Acute Leukemia Research Group, Department of Clinical Science, University of Bergen, Jonas Lies vei 91, 5009 Bergen, Norway; elise.aasebo@helse-bergen.no (E.A.); hakon.reikvam@uib.no (H.R.)

³ Section for Hematology, Department of Medicine, Haukeland University Hospital, 5009 Bergen, Norway

⁴ Department of Physical Chemistry, University of Granada, Avenida de la Fuente Nueva S/N, 18071 Granada, Spain

⁵ Instituto de Investigación Biosanitaria ibs.GRANADA, 18012 Granada, Spain

* Correspondence: oystein.bruserud@helse-bergen.no

Abstract: Acute myeloid leukemia (AML) is an aggressive bone marrow malignancy that can be cured only by intensive chemotherapy possibly combined with allogeneic stem cell transplantation. We compared the pretreatment proteomic profiles of AML cells derived from 50 patients at the time of first diagnosis with normal CD34⁺ bone marrow cells. A comparison based on all AML and CD34⁺ normal cell populations identified 121 differentially abundant proteins that showed at least 2-fold differences, and these proteins included several markers of neutrophil differentiation (e.g., TLR2, the integrins ITGM and ITGX, and downstream mediators including RHO GTPase, S100A8, S100A9, S100A22). However, the expression of these 121 proteins varied between patients, and a subset of 28 patients was characterized by increased long-term AML-free survival, signs of myeloid AML cell differentiation, and favorable genetic abnormalities. These two main patient subsets (28 with differentiation versus 22 with fewer signs of differentiation) also differed with regard to the phosphorylation of 16 differentially abundant proteins. Furthermore, we also classified our patients based on their expression of 16 proteins involved in the regulation of iron metabolism/ferroptosis and showing differential expression when comparing AML cells and normal CD34⁺ cells. Among the 22 patients with less favorable prognosis, we could then identify a genetically heterogeneous subset characterized by adverse prognosis (i.e., death from primary resistance/relapse) and an iron metabolism/ferroptosis protein profile showing similarities with normal CD34⁺ cells. We conclude that proteomic profiles differ between AML and normal CD34⁺ cells; especially, proteomic differences reflecting differentiation and regulation of iron metabolism/ferroptosis are associated with risk of relapse after intensive conventional therapy.

Keywords: acute myeloid leukemia; normal CD34⁺ bone marrow cells; hematopoiesis; differentiation; integrin; Toll-like receptor; patient heterogeneity; intracellular signaling; cellular communication; proteomics; mass spectrometry



Academic Editor: Vikram Sharma

Received: 2 January 2025

Revised: 5 February 2025

Accepted: 14 February 2025

Published: 17 February 2025

Citation: Selheim, F.; Aasebø, E.; Reikvam, H.; Bruserud, Ø.; Hernandez-Valladares, M. Proteomic Comparison of Acute Myeloid Leukemia Cells and Normal CD34⁺ Bone Marrow Cells: Studies of Leukemia Cell Differentiation and Regulation of Iron Metabolism/Ferroptosis. *Proteomes* **2025**, *13*, 11. <https://doi.org/10.3390/proteomes13010011>

Copyright: © 2025 by the authors. Licensee MDPI, Basel, Switzerland. This article is an open access article distributed under the terms and conditions of the Creative Commons Attribution (CC BY) license (<https://creativecommons.org/licenses/by/4.0/>).

1. Introduction

Acute myeloid leukemia (AML) is an aggressive malignancy characterized by the proliferation of immature leukemia cells in the bone marrow [1]. Its incidence increases with age [1–3], and the only potentially curative treatment is intensive chemotherapy

possibly combined with allogeneic hematopoietic stem cell transplantation (allo-HSCT) [2]. However, such treatment is not possible for unfit patients and in the large group of elderly patients due to the unacceptable risk of severe or fatal toxicities [4–6]. Thus, there is a need for new therapeutic strategies to improve both the survival of younger patients with resistant/relapsed AML and elderly/unfit patients with a high risk of severe toxicity [2,4–6]. New targeted therapies are therefore tried in the treatment of AML [4–9].

AML is a heterogeneous malignancy with regard to AML cell morphology/differentiation, genetic abnormalities, and communication with neighboring nonleukemic cells in the bone marrow [1,2]. This heterogeneity is the basis for the subclassification of AML described in the WHO 2022 classification [1]. Despite the heterogeneity, there are also fundamental common biological characteristics, e.g., bone marrow homing, limited signs of AML cell differentiation, and rapid progression without treatment [1]. These last characteristics justify the therapeutic similarities between the various patient subsets when using conventional intensive chemotherapy as well as allo-HSCT [2]; the only exception being the acute promyelocytic (APL) variant [2].

The aim of this present study was to characterize the molecular consequences of AML transformation by comparing primary AML cells with normal CD34⁺ bone marrow cells, i.e., a normal counterpart for this bone marrow malignancy that also shows limited differentiation [10–15]. Furthermore, the acceptable intensity of AML therapy is determined by the balance between antileukemic efficiency versus the risk of severe/fatal toxicity, especially hematological toxicity, which is often dose-limiting and contributes to treatment-related mortality [2,4,16–20]. One hypothesis could then be that an unfavorable balance between anti-AML efficiency versus the risk of severe/lethal hematological toxicity for certain therapeutic approaches is due to biological similarities between normal and leukemic hematopoietic cells [20,21]. We would also expect proteomic differences between normal and leukemic hematopoietic cells to reflect fundamental AML cell characteristics and important mechanisms involved in leukemogenesis and possibly also chemoresistance against conventional as well as new targeted therapies [2,22,23]. Finally, proteomic profiling may become an alternative strategy for the evaluation of differentiation in AML cells. In this context, we performed a preliminary/pilot study where we investigated whether proteins showing differential expression when comparing normal and leukemic hematopoietic cells can be used for patient subclassification and the identification of patient subsets that differ in prognosis/survival after conventional intensive therapy. The present results suggest that our identification of distinct patient subsets is relevant for the prognostication of AML patients receiving conventional intensive chemotherapy, but this needs to be further investigated and confirmed in larger clinical studies.

2. Materials and Methods

2.1. Patient and Cell Samples

We reanalyzed a previous liquid chromatography with tandem mass spectrometry (LC–MS/MS)-characterized proteomic cohort including AML cells from 50 Caucasian patients with non-APL variants of AML at the time of first diagnosis (Table 1) [24]. This study included (i) all consecutive patients (acute promyelocytic leukemia being excluded) from the same geographical area during a defined time period (1995–2012) and receiving intensive conventional AML therapy (ii) with a high percentage of AML blasts among circulating leukocytes (see below) who (iii) completed the planned intensive and potentially curative antileukemic treatment. All patients had >20% AML cells among nucleated bone marrow cells. The patient cohort did not include patients with the uncommon erythroid and megakaryocytic AML variants.

Table 1. A summary of important clinical and biological characteristics of the 50 AML patients included in this present study.

Age (median, range, and IQR)	55 years (18–80) IQR: 60 – 41 = 19	Cytogenetics (number)	Favorable 6 Intermediate 7 Adverse 8 Normal 26 Unknown 3
Sex (male/female, number)	27/23		
Secondary AML (number)	Chemotherapy 3 MDS 2	FLT3-ITD (number) ² FLT3-TKD mutation (number) ² NPM1 insertion (number)	12 4 15
FAB classification (number)	M0 6 M1 9 M2 8 M4 15 M5 12	ELN 2022 classification	Favorable 14 Intermediate 5 Adverse 13 Intermediate/adverse 12 ³ Unclassified 6 ³
CD34 positivity (number) ¹	29		

¹ CD34 positivity defined as $\geq 20\%$ positive cells by flow cytometry; four patients not examined. ² Three patients not tested for *FLT3-ITD*, five not tested for *FLT3-TKD* mutation, and three not tested for *NPM1* insertions (TKD, tyrosine kinase domain). ³ Extended mutational analyses were available only for 26 of the 50 patients. The group intermediate/adverse prognosis means that these patients did not fulfill any of the ELN criteria for favorable prognosis but they were not examined in an extended mutational analysis with regard to additional adverse mutation as defined by ELN [2]. Unclassified means that the patients were examined neither for all ELN-defined favorable prognostic factors nor for additional adverse prognostic mutations in an extended analysis (i.e., missing karyotype or *NPM1/FLT3/CEBPA* analyses).

None of the patients received autologous stem cell transplantation. Some patients received allogeneic stem cell transplantation according to national Norwegian guidelines; the time for allotransplantation is indicated in Tables S8 and S13.

The patients were classified according to the 2022 ELN risk classification by genetics at initial diagnosis [2] (Table 1). Only 26 patients were investigated with an extended panel of AML-associated mutations, and for this reason, 11 patients were classified as intermediate/adverse (i.e., absence of favorable genetic abnormalities) or unclassified (missing karyotyping or analysis of *NPM1/FLT3/CEBPA* genetic abnormalities).

Enriched primary AML cells could be prepared by density gradient separation alone from peripheral blood; all patients had $\geq 80\%$ AML blasts among circulating leukocytes, and gradient-separated cells therefore included $\geq 95\%$ AML blast cells. After gradient separation, the AML samples were cryopreserved according to a standardized protocol [25] and stored in liquid nitrogen until use. Briefly, cells were dissolved in standardized RPMI 1640 culture medium (Stem Cell Technologies, Vancouver, BC, Canada) supplemented with 40% heat-inactivated fetal calf serum (FCS) (Stem Cell Technologies) before being placed on ice; thereafter, an equal volume of cold medium with 20% dimethylsulfoxide (DMSO) was gradually added over 5 min to reach the final concentrations of FCS 20% and DMSO 10%. The cells were thereafter transferred to storage for 24–72 h at $-70\text{ }^{\circ}\text{C}$ before being transferred to liquid nitrogen. Cells were thawed at $0\text{ }^{\circ}\text{C}$ and immediately transferred to the proteomic solution (see also Section 2.2) [24,26].

Cryopreserved normal CD34⁺ bone marrow cells were derived from eight healthy Caucasians (four men and four women; PromoCell GMBH; Heidelberg, Germany); their age did not differ from the AML patients (median age, 50.5 years; range, 41–55 years; interquartile range (IQR), 50.5 – 43.25 = 7.25). These cells were also cryopreserved in 10% DMSO. The proteomic analyses of the normal CD34⁺ cells have not been published previously but are available at ProteomeXchange, data identifier PXD058846.

2.2. Proteomic Analysis

Our methods have been described in detail previously [24,26,27], and we thus tested several sample preparation workflows [27]. These experiments included double versus single-digestion and in-solution versus filter-based digestions for proteome analysis, metal oxide affinity chromatography (MOAC), immobilized metal affinity chromatography (IMAC), and sequential elution from IMAC (SIMAC) for phosphoproteome analysis [28–31]. The results showed that FASP procedures produced the highest number of quantified proteins with a reduced number of missed cleavages. IMAC was selected because it produced the highest number of quantified phosphopeptides, even though MOAC, IMAC, and SIMAC protocols isolated different phosphoproteoforms.

Quantitative proteomics of the AML patients and CD34⁺ cells was performed according to the label-free quantification (LFQ) approach. Proteome extraction was carried out in 4% sodium dodecyl sulfate (SDS) and 0.1 M Tris-HCl (pH 7.6) with immediate boiling to inactivate proteases and phosphatases. Samples were reduced with 0.1 M of dithiothreitol (DTT) and alkylated with 50 mM iodacetamide (IAA) before being digested in a filter unit according to the filter-aided sample preparation (FASP) procedure, adding trypsin to 50 mM ammonium bicarbonate in a 1:50 ratio [32,33]. Quantitative phosphoproteomics was carried out with samples spiked with a super-SILAC (stable isotope labeling by amino acids in cell culture) mix [34]. The phosphoproteomics samples were FASP-processed and enriched for phosphopeptides using the IMAC approach [24]. LC–MS/MS runs were carried out with a Q Exactive HF Orbitrap mass spectrometer coupled to an Ultimate 3000 Rapid Separation liquid chromatography (LC) system. LC–MS/MS methods have been described in detail previously as Supplementary Information [24]. In brief, LC–MS/MS raw files for primary AML cells and normal CD34⁺ bone marrow cells were processed with MaxQuant software (version 1.5.2.8). The spectra were searched against the concatenated reverse-decoy Swiss-Prot Homo sapiens database (downloaded on 5 November 2015) utilizing the Andromeda search engine. Relative label-free quantification was performed using the MaxLFQ algorithm [35], with the LFQ count set to 1. This algorithm normalizes protein intensities based on peptide ratios measured in all pairwise comparisons within the entire sample batch. The MaxQuant parameters were configured as follows: cysteine carbamidomethylation was set as a fixed modification, while methionine oxidation, protein N-terminal acetylation, and Gln→pyro-Glu were included as variable modifications. Trypsin was stated as the digestion protease. The false discovery rate (FDR) was set at 0.01 for both peptides and proteins, and a minimum peptide length of six amino acids was required. Additionally, the match-between-runs and re-quantify options were enabled.

All proteomic raw data and MaxQuant output files together with the phosphoproteomic raw data can be found in the ProteomeXchange consortium with the dataset identifiers PXD014997 and PXD058846.

2.3. Morphological, Cell Surface Marker and Genetic Subclassification of AML Patients

The FAB classification is regarded as a standardized and well-described system to characterize and classify patients with regard to AML cell differentiation [36,37]. In our present study, we defined monocytic differentiation as FAB-M4/M5, neutrophil differentiation as FAB-M2, and undifferentiated as FAB-M0/M1. No erythroid or megakaryocytic variants (i.e., FAB-M6/M7 AMLs) were included.

Cell surface markers were analyzed with flow cytometry and the karyotype with standard cytogenetic analysis. Analyses of FLT3 and NPM1 mutations have been described previously [38]. Submicroscopic mutational profiling of 54 genes frequently mutated in AML was performed using the Illumina TruSight Myeloid Gene Panel and sequenced using the MiSeq system and reagent kit v3 (Illumina, San Diego, CA, USA) [38].

2.4. Statistical and Bioinformatical Analyses

Our various bioinformatical analyses are summarized in the flow chart in Figure 1.

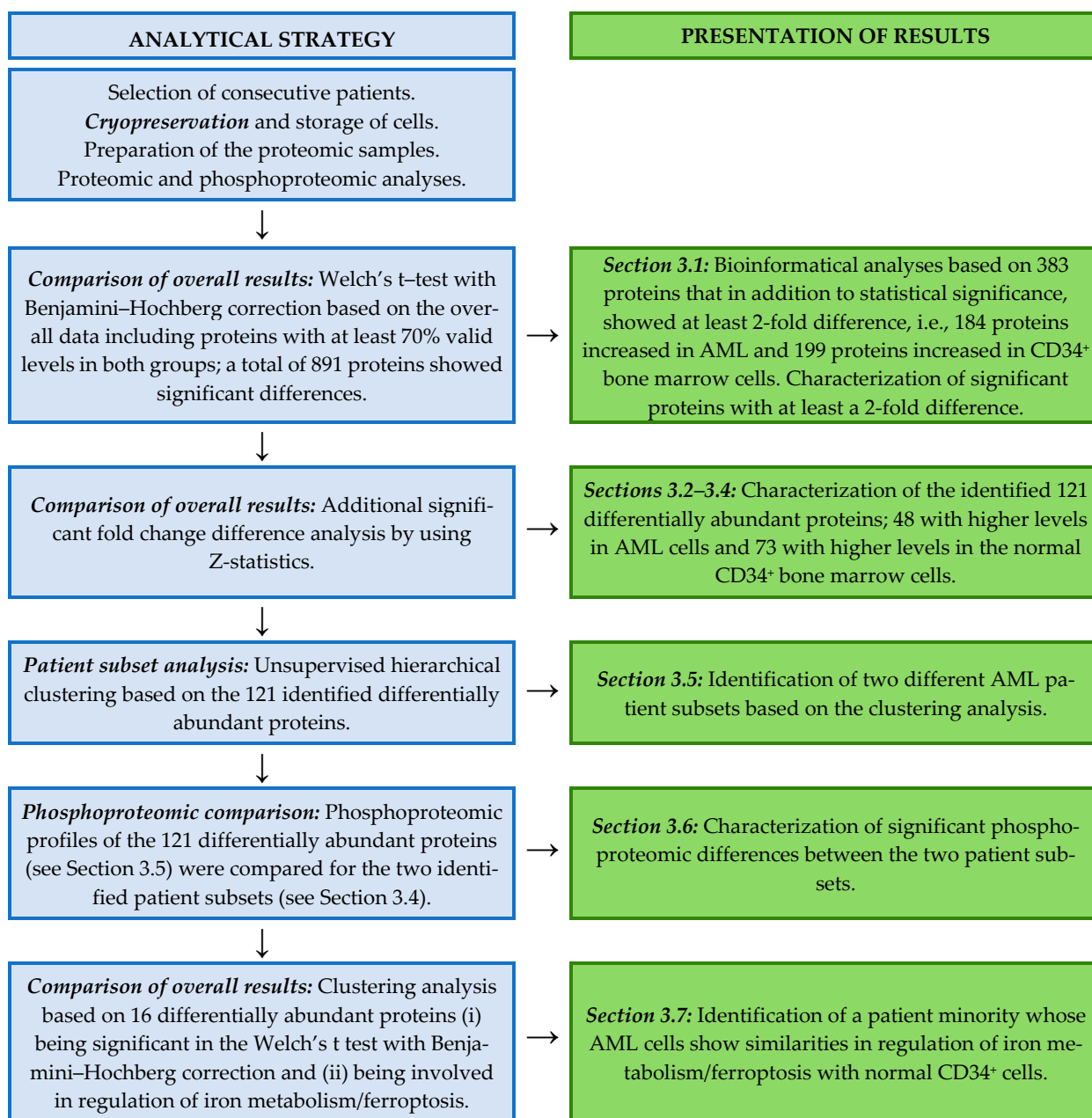


Figure 1. A flow chart showing the various statistical/bioinformatical analyses in this present study and the corresponding presentation of the results in the various subsections of Results.

The Perseus 2.0.7.0 platform was used for functional and statistical analyses of proteomics and phosphoproteomics data [39]. Patient subset data were normalized by using width adjustment. A Welch's *t*-test with Benjamini-Hochberg correction (i.e., FDR < 0.01) was performed to test for significant difference between means of compared groups. Z-statistics were carried out on the Welch's *t*-test regulated proteins to identify proteins with significantly different fold changes [40]. A flow chart summarizing the various bioinformatical analyses and their presentation in our study is given in Figure 1.

Welch's *t*-test with *p*-value < 0.05 was performed to test for significantly differentiated phosphorylation sites between compared groups. Reactome pathway, Gene Ontology (GO), and KEGG pathway enrichment analyses were obtained with the Enrichr gene set search

engine [41–44]. Protein–protein interaction (PPI) network analyses were performed with the STRING database version 11.5. Networks were visualized using the Cytoscape platform v3.10.0 [45]. GraphPad v8.0.1 and the Perseus platform were used to make the volcano plot and the heatmap, respectively.

3. Results

3.1. Primary AML Cells at the Initial Diagnosis Show Increased Abundance of Several Neutrophil Differentiation Biomarkers Compared with Normal CD34⁺ Bone Marrow Cells; Results from an Initial Statistical Comparison

The total proteomic profiles for all 50 AML patients and eight normal CD34⁺ bone marrow cell populations were compared. We first used Welch's *t*-test with Benjamini–Hochberg correction (i.e., FDR < 0.01) based on only those proteins with at least 70% valid values both for leukemic and normal cells. A total of 891 proteins showed a statistically significant difference (i.e., *p* < 0.05); this included 184 proteins with at least a 2-fold median increase for the AML cells (Table S1) and 199 proteins showing at least a 2-fold increase for the CD34⁺ normal bone marrow cells (Table S2).

The 10 top-ranked Reactome terms for the 184 significant proteins with at least 2-fold increased levels in AML cells are listed in Table S3 together with the corresponding differentially abundant proteins for each of these terms. The terms reflecting neutrophil differentiation/innate immunity included a relatively large number of overlapping proteins, whereas fewer proteins were included in terms reflecting integrin function, endothelial cell function, and RHO signaling, respectively. There was a considerable overlap of proteins between each of these last minor groups and the terms reflecting neutrophil functions/innate immunity. These top 10 Reactome terms included 79 of the 184 proteins with increased levels in the AML cells.

The top-ranked Reactome terms for the 199 proteins with an at least 2-fold increase in normal CD34⁺ bone marrow cells reflected nucleotide metabolism/synthesis (purine ribonucleotide monophosphate biosynthesis, metabolism of nucleotides, nucleotide biosynthesis), regulation of DNA functions/mitosis (DNA strand elongation, activation of pre-replicative complex, mitotic G1 phase, and G1/S transition), and integrin signaling (p130CAS linkage to MAPK signaling for integrins, BRB2:SOS provides linkage to MAPK signaling for integrins) (Table S4). However, these terms included only 33 of the 199 proteins with high levels in the CD34⁺ cells.

We conclude that the differentially abundant protein identified in this initial comparison of AML and normal CD34⁺ cells shows extensive biological diversity. The main difference was that proteins with increased levels in AML cells mainly reflected limited myeloid/neutrophil differentiation, whereas proteins with increased levels in normal CD34⁺ cells reflected a different regulation of cellular proliferation and integrin-associated intracellular MAPK signaling.

3.2. Proteomic Comparison of AML Cells at Initial Diagnosis and Normal CD34⁺ Bone Marrow Cells: High Expression of Neutrophil Markers in the AML Cells and High Levels of Platelet/Coagulation Biomarkers in Normal Cells

Our initial strategy was the comparison of the protein levels for all 50 AML patients and the eight normal CD34⁺ bone marrow cell populations by using Welch's *t*-test with Benjamini–Hochberg correction (i.e., FDR < 0.01) as described in Section 3.1. As an alternative and additional statistical strategy to our previous use of a fold change cut-off value (i.e., 2-fold; see Section 3.1) we conducted a significant fold change difference analysis (*Z*-statistics) of the 891 proteins identified in the initial step analysis described in Section 3.1. By using this approach, we identified only 48 proteins with significantly increased levels in AML cells and 73 proteins with increased levels in the normal CD34⁺ bone marrow cell

populations (Table S5; see also Figure 2); all these proteins were among the most significant in Welch’s *t*-test with Benjamini–Hochberg correction (as indicated in Tables S1 and S2).

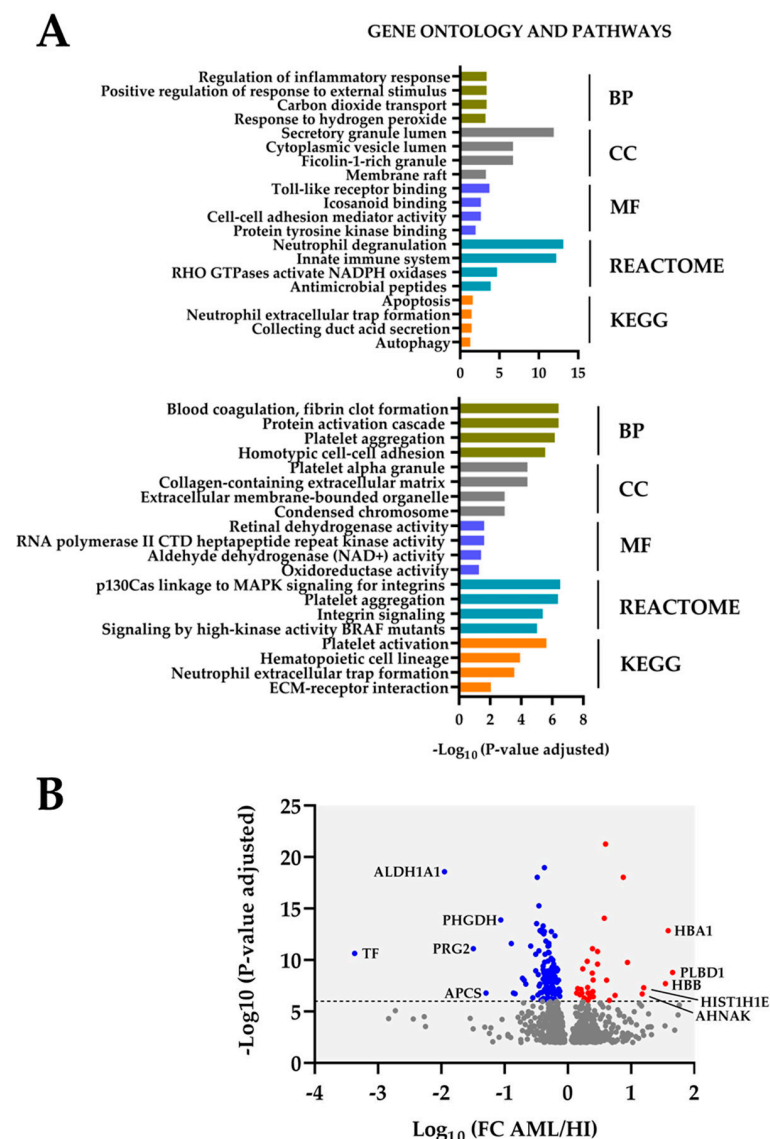


Figure 2. Proteomic differences between primary AML cells derived from 50 patients and normal CD34⁺ bone marrow cells derived from eight healthy individuals. A total of 891 differentially abundant proteins were identified in the initial statistical analysis but only 121 of these proteins showed significant fold change differences (Z-statistics). The analyses presented in the figure are based on these 121 proteins. **(A)** The figure presents the Gene Ontology (GO), Reactome, and KEGG analyses for the 48 (upper plot) and 73 (lower plot) proteins that showed increased and decreased (i.e., increased in normal CD34⁺ cells) levels in primary AML cells, respectively. **(B)** The volcano plot is based on all 891 differentially abundant proteins. The colored dots represent proteins with adjusted *p*-values < 1 × 10^{−6} (see the y-axis); red dots represent increased levels in primary AML cells (i.e., AML cell/CD34⁺ cell > 1.0); blue dots represent proteins with increased levels in the normal CD34⁺ bone marrow cells. Abbreviations: BP, biological process; CC, cellular compartment; FC, fold change; MF, molecular function.

Reactome analysis (Figure 2A) of the 48 AML-associated proteins showed enrichment of proteins reflecting neutrophil degranulation (21 proteins) and innate immunity (17 overlapping proteins). The cellular compartment (CC) GO terms also reflected differences consistent with neutrophil differentiation, i.e., granular/vesicular lumen. Furthermore, the top four Reactome terms for the AML cells also included the terms RHO GTPases activate NADPH oxidases (four proteins) and antimicrobial peptides (five proteins) (Figure 3).

The top-ranked terms from the other GO term analyses (biological process, BP; molecular function, MF) and the KEGG analysis showed lower significance than the Reactome/CC terms (Figure 2A).

Neutrophil degranulation–Innate immune system	RHO GTPases activate NADPH oxidases	Antimicrobial peptides	Platelet aggregation, Integrin signaling	Fold change AML cells/Normal CD34 ⁺ cells (log ₂)	Fold change significance	Gene name	Protein name
Yellow	Green			5.80	0.0002	NCF1	Neutrophil cytosol factor 1/1B/1C
Yellow				4.39	0.0029	SIRPA	Tyrosine-protein phosphatase non-receptor type substrate 1
Yellow	Green	Green		3.99	0.0058	S100A8	Protein S100-A8
Yellow	Green			3.94	0.0063	PRKCD	Protein kinase C delta type
Yellow				3.88	0.0068	ITGAX	Integrin alpha-X
Yellow		Green		3.77	0.0082	TLR2	Toll-like receptor 2
Yellow	Green	Green		3.61	0.0104	S100A9	Protein S100-A9
Yellow		Green		3.59	0.0108	BPI	Bactericidal permeability-increasing protein
Yellow				3.50	0.0124	CD180	CD180 antigen
Yellow				3.34	0.0155	ATG7	Ubiquitin-like modifier-activating enzyme ATG7
Yellow				3.42	0.0139	ITPR1	Inositol 1,4,5-trisphosphate receptor type 1
Yellow				3.23	0.0181	ITGAL	Integrin alpha-L
Yellow				3.13	0.0208	ANXA2	Annexin A2
Yellow				3.02	0.0244	MNDA	Myeloid cell nuclear differentiation antigen
Yellow				2.92	0.0279	S100A11	Protein S100-A11
Yellow				2.86	0.0301	GNS	N-acetylglucosamine-6-sulfatase
Yellow				2.73	0.0353	GRN	Granulins (1/2/3/4/5/6/7)
Yellow				2.70	0.0366	APAF1	Apoptotic protease-activating factor 1
Yellow		Green		2.63	0.0403	LYZ	Lysozyme C
Yellow				2.54	0.0446	SERPINA3	Alpha-1-antichymotrypsin
Yellow				2.54	0.0450	ATP6V0D1	V-type proton ATPase subunit d 1
			Purple	-3.14	1.48 × 10 ⁻⁵	ITGA2B	Integrin alpha-IIb
			Purple	-3.14	1.47 × 10 ⁻⁵	GP1BA	Platelet glycoprotein Ib alpha chain
			Purple	-4.03	1.44 × 10 ⁻⁸	FGG	Fibrinogen gamma chain
			Purple	-4.12	6.74 × 10 ⁻⁹	FGB	Fibrinogen beta chain
			Purple	-4.36	7.33 × 10 ⁻¹⁰	FGA	Fibrinogen alpha chain
			Purple	-8.11	<10 ⁻¹⁵	FN1	Fibronectin

Figure 3. Proteomic comparison of proteins being statistically significant both in the initial Welch’s *t*-test analysis with at least a 2-fold difference and also in the additional AML cell/normal CD34⁺ bone

marrow cell fold change comparison (Z-statistics, $p < 0.05$)—an overview of proteins included in the top-ranked Reactome terms (see Figure 2A,B). The Reactome terms are given at the top of the figure. The left part of the figure shows the proteins included in the two overlapping terms neutrophil degranulation (R-HSA-6798695, 21 proteins) and innate immune system (R-HAS-168249, 17 overlapping proteins), presented in yellow as a single column, and the two terms (left middle) RHO GTPases activate NADPH oxidase (middle-left, R-HAS-5668599) and antimicrobial peptides (middle-right R-HAS-6803157) presented in green. All these terms were enriched in the primary AML cells. The right column in purple shows all proteins with increased levels in normal CD34⁺ cells and included in the overlapping Reactome terms p130Cas linkage to MAPK signaling for integrins R-HAS-372708, platelet aggregation (plug formation) R-HAS-76009, integrin signaling R-HAS-354192, and signaling by high-kinase activity BRAF mutants R-HAS-6802948 (see Figure 2A).

The analyses of normal CD34⁺ bone marrow cells reflected increased levels of a relatively small number of proteins involved in coagulation/platelet activation; the four top-ranked Reactome terms included a total of six proteins out of the seventy-three significantly increased proteins in CD34⁺ cells (Figure 3). The terms identified by GO, Reactome, and KEGG analyses of these 73 proteins showed generally lower significance than the Reactome/CC terms for the AML cells (Figure 2).

Based on these analyses, our conclusion is the same as for the analysis described after the first statistical analysis described in Section 3.1—differentially abundant proteins between AML and normal CD34⁺ cells show large biological diversity with the main characteristic being an increased expression of proteins reflecting limited myeloid/neutrophil differentiation of the AML cells, whereas the increased levels of regulators of the proliferation/cell cycle possibly reflect the immature/stem cell status of the CD34⁺ cells.

3.3. Analysis of Differentially Abundant Proteins by Volcano Plot Analysis; Identification of Neutrophil Differentiation Markers as Well as Regulators of Cellular Metabolism Including Iron Metabolism

We conducted a volcano plot analysis of the 121 differentially abundant proteins identified after the fold change significance analysis (Figure 2B). Only ten biologically diverse proteins (five increased in AML and five in CD34⁺ cells) showed a marked differential expression, including myeloid differentiation markers (HBA1, HBB, PRG2, and possibly the antimicrobial PRGT); regulators of lipid (ALDH1A1, PLBD1), amino acid (PHGDH, possibly APCS), and iron (TF) metabolism; and transcriptional regulators (HIST1H1E, possibly APCS) (Table S6). Thus, this analysis also identified several differentiation markers but, in addition, a few metabolic and functional DNA/transcriptional regulators.

3.4. Analysis of Protein–Protein Interaction Networks; Identified Networks Involve Regulators of Intracellular Signaling, Platelet Function, and Iron Metabolism, as Well as Transcription and DNA Repair

Protein–protein interaction (PPI) network analyses based on the 121 differentially abundant proteins from the fold change significance analysis identified only four networks with at least three members (Figure 4):

- *Regulation of MAPK cascade.* This network included nine proteins, three of them showing increased levels in primary AML cells. Differences in regulators of integrin-associated MAPK regulators were also identified in our first global analysis (see first Section 3.1 of Results and Table S4, right columns).
- *Nitric oxide transport.* The network included the two hemoglobin chains also identified in the volcano plot together with the hemoglobin-binding protein haptoglobin.
- *Base excision repair.* This network included three proteins with decreased levels in AML cells.

- *Aldehyde dehydrogenase*. This network included three proteins with decreased levels in AML cells.

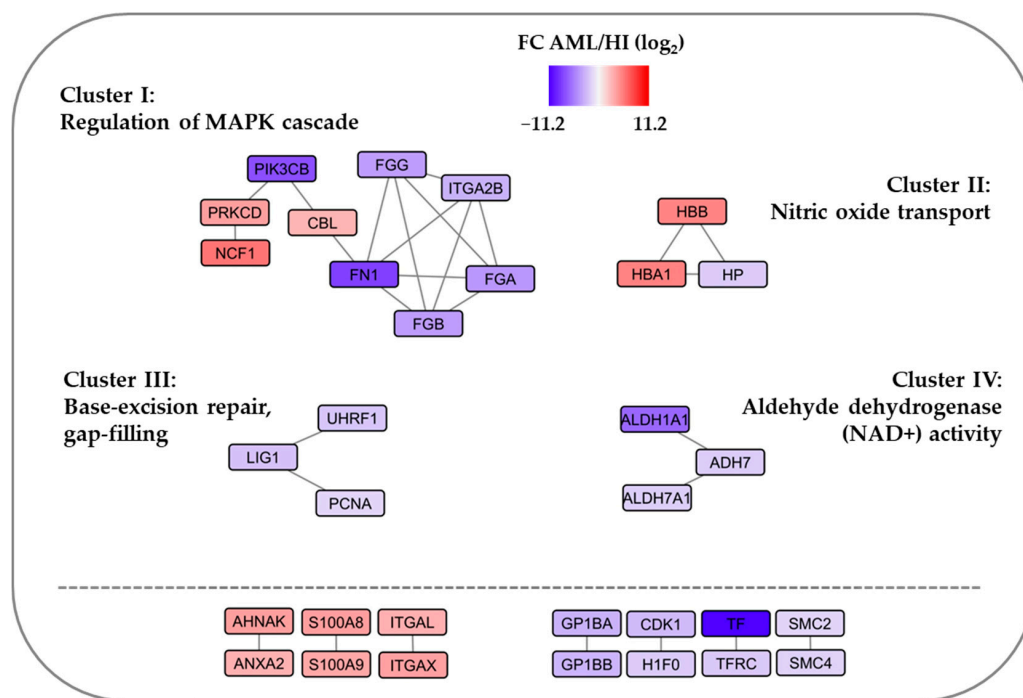


Figure 4. Significant protein–protein interaction networks (**upper part**) and pairs (**lower part**) identified based on the analysis of 121 regulated proteins showing fold change (FC) significance between primary AML cells derived from 50 patients and normal CD34⁺ bone marrow cells derived from eight healthy individuals.

Thus, only one relatively large network was identified, suggesting that the intracellular molecular context of MAPK signaling is different for primary AML cells compared with normal CD34⁺ bone marrow cells. Only 18 out of 121 differentially abundant proteins were included in these four networks.

We identified seven additional pairs of interacting proteins. Three pairs included proteins that were increased in the AML cells, including (i) one pair with two integrin alpha chains and (ii) two pairs with three proteins (S100A8, S100A9, and AHNAK) involved in signaling/calcium metabolism. Furthermore, four pairs were decreased in AML cells, and these are referred to as platelet-associated proteins (GP1BA and GP1BB), iron metabolism (transferrin and its receptor), cell cycle/histone regulation (CDK1, H1F0), and two members of the family structural maintenance of chromosomes (SMC) that modulate chromosome structure during mitosis (SMC2, SMC4). However, only 33 of the 121 proteins were included in interacting networks/pairs, an observation suggesting that the identified 121 proteins show a considerable biological heterogeneity.

3.5. Even Proteins Showing Strong Differential Abundance When Comparing AML and CD34⁺ Cells, in General, Vary Between Individual Patients and Can Be a Basis to Identify AML Patient Subsets

We conducted an unsupervised hierarchical clustering analysis based on the 121 differentially abundant proteins identified after Z-statistics (Figure 5). The differentially abundant proteins were separated into two main clusters (see left part of the figure, referred to as platelet activation and neutrophil degranulation, respectively), and both main clusters could be further subdivided into two subclusters. The upper main cluster included those proteins that reflected platelet activation/function in the Reactome analysis (Figure 2A; Table S6), and all these proteins were located in the lower subcluster (Table S7). On the other

hand, the lower main protein cluster included the large majority of proteins reflecting the terms neutrophil degranulation/innate immune system, RHO GTPases activate NADPH oxidases and antimicrobial peptides in the Reactome analysis (Figure 2B, Table S6), and the large majority of these proteins were included in the lower subcluster (Table S7).

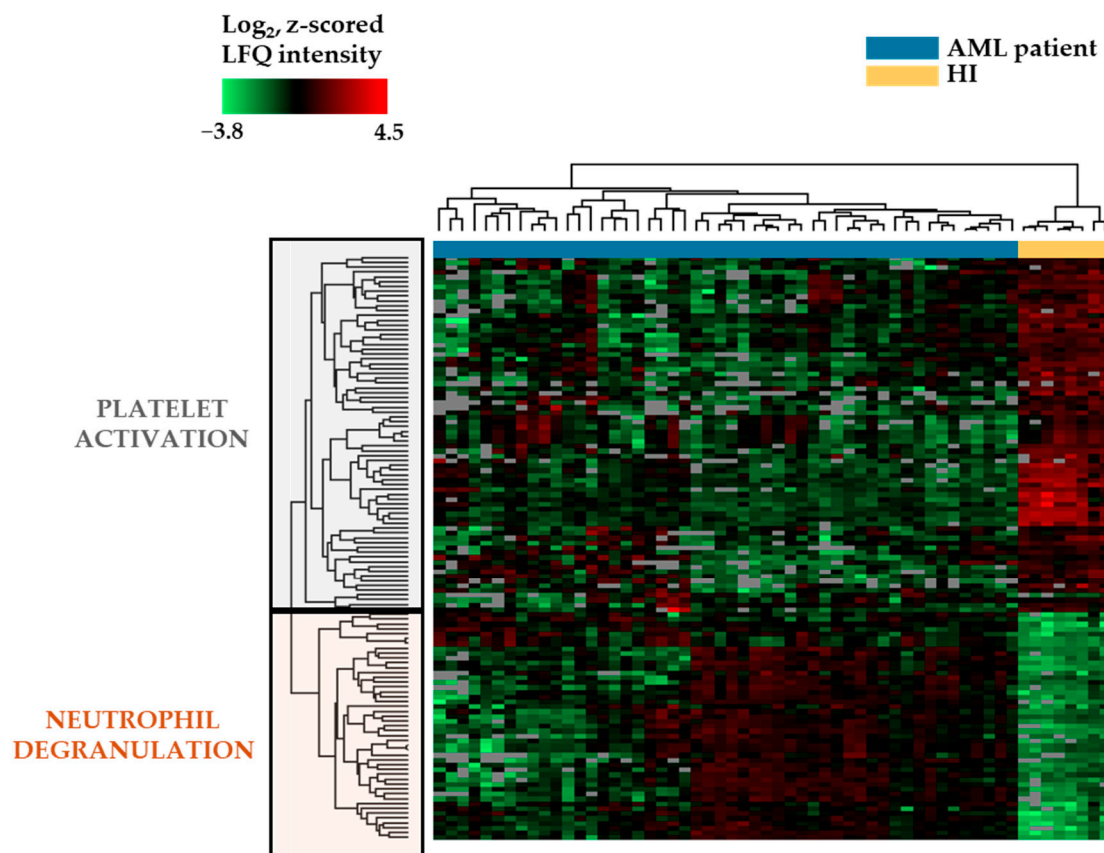


Figure 5. Hierarchical clustering analysis based on the proteomic profile for primary AML cells derived from 50 patients and eight CD34⁺ bone marrow cell populations derived from healthy individuals (HI). The clustering of normal and leukemic cells is shown at the top of the figure; the clustering of the 121 differentially abundant proteins after analysis of fold change significance (Z-statistics) is shown in the left part of the figure. The ranking of patients from left to right is presented in Table S7 and the ranking of the proteins from the top to bottom is presented in Table S8. The two main protein clusters are referred to as platelet activation and neutrophil degranulation due to their inclusion of proteins classified in Reactome terms that reflect these processes (see Tables S6 and S7).

The normal CD34⁺ bone marrow cell samples formed a separate main cluster in this analysis; see the top of Figure 5 to the right. The primary AML cell samples formed the large left main cluster that could be further subdivided into several subclusters. Furthermore, this analysis showed that patients could be divided into two main subsets based on the expression of a subset of proteins showing generally high levels when comparing the total AML and CD34⁺ cell populations (the lower protein main cluster; see left part of Figure 5). The 22 patients on the left showed a generally lower expression of these proteins compared with a higher expression in the 28 patients on the right.

The clinical and biological characteristics of these two patient subsets are presented in Table S8 and are compared/summarized in Table S9. The 28-patient subset on the right had a significantly lower age (Table S9; Fisher's exact test, $p = 0.00076$), a lower frequency of undifferentiated FAB-M0/M1 leukemic cells ($p = 0.0003$), a lower frequency of CD34⁺ AML cell populations ($p = 0.0307$), higher frequencies of favorable ($p = 0.0312$) and favorable/normal karyotypes ($p = 0.0299$), a lower frequency of refractory/relapsed

disease ($p = 0.0365$), and a higher frequency of long-term AML-free survival ($p = 0.0016$) compared with the 22-patient subset on the left. These associations are mainly caused by several patients with a favorable karyotype (i.e., $\text{inv}(16)$) who clustered close to each other among the 28-patient subset on the right.

We compared the two clusters with regard to peripheral blood blast count and the percentage of AML blast cells among the nucleated bone marrow cells. The 28 patients in the neutrophil degranulation/differentiation cluster showed a significantly higher peripheral blood blast count (median $42.5 \times 10^9/\text{L}$, range $4\text{--}357 \times 10^9/\text{L}$, IQR $71.0 - 29.5 = 41.5 \times 10^9/\text{L}$) than the other 22 patients (median $23 \times 10^9/\text{L}$, range $5\text{--}231 \times 10^9/\text{L}$, IQR $47.25 - 10.75 = 36.5 \times 10^9/\text{L}$; Mann–Whitney U test, $p = 0.026$). In contrast, the percentage of bone marrow blasts did not differ between the 28 neutrophil differentiation patients (median 76.5%, range 30–97%, IQR $85.75 - 60.50 = 25.25$) and the other 22 patients (median 83.5%, range 25–99%, IQR $95.00 - 58.25 = 35.25$).

Cryopreservation and storage in liquid nitrogen can lead to a reduced abundance of membrane molecules [46]. Several of the identified neutrophil differentiation markers included in the clustering analysis are cell surface molecules. We, therefore, compared the cell storage times for the left 22-patient main cluster (median 86 months, range 60–240 months, IQR $139 - 66 = 73$ months) and the right 28-patient main cluster with the neutrophil differentiation patients (median 131 months, range 60–245 months, IQR $225.00 - 72.25 = 152.25$ months). This difference was not statistically significant.

3.6. Additional Phosphoproteomic Differences of the 121 Differentially Abundant Proteins from the AML/CD34⁺ Cell Comparison: A Comparison of the Two Patient Subsets Identified in the Proteomic Clustering Analysis of These 121 Proteins

Primary AML cells derived from 41 of the 50 patients were included in a previous phosphoproteomic study [24]; 23 of these patients belonged to the larger main subset (Figure 5, the 28 patients on the right) and the other 18 patients belonged to the smaller main subset (Figure 5, the 22 patients on the left). We observed detectable phosphorylation for 38 of the 121 differentially abundant proteins identified in our proteomic comparison of primary AML cells and normal CD34⁺ bone marrow cells (i.e., proteins with a fold difference exceeding 2.0; see above). These 38 proteins had 174 detectable phosphorylated sites. Next, we conducted a statistical comparison (Welch's t -test) of the phosphorylation level for these 174 phosphosites/38 differentially abundant proteins between the two patient subsets identified in the unsupervised hierarchical clustering analysis presented in Figure 5 (i.e., 23 of the 28 right patients versus 18 of the 22 left patients; see first chapter of this section). This analysis identified a total of 53 differentially phosphorylated sites in 16 proteins that differed significantly between these two patient subsets. These differing phosphosites are presented in Tables 2 and S10; important characteristics of the 16 phosphoproteins are presented in Table S11.

Table 2. Protein phosphorylation of primary human AML cells derived from two patient subsets (see Figure 5); the identification of protein phosphorylation sites that (i) were detected in a subset of the 121 differentially abundant proteins (i.e., 38 proteins) that showed at least a 2-fold difference when comparing the levels in AML cells and normal CD34⁺ cells; (ii) in addition, a statistically significant difference when each identified phosphosite was compared between the two patient subsets identified in the clustering analysis is presented in Figure 5 (i.e., 23/28 right versus 18/22 left patients). The first criterion (i) identified 174 phosphosites in 38 of the 121 differentially abundant proteins; 53 of these phosphosites in 16 of the differentially abundant proteins also fulfilled the second criterion (ii) and are listed in the table. The table presents the gene name, protein name, number of phosphosites, and the possible functional importance of the protein phosphorylation status for each of these 16 proteins. The gene names for proteins showing increased levels in normal CD34⁺ cells are underlined and marked in *italics* (see the left column).

Gene Name	Protein Name	Number of Sites	Effects of Protein Phosphorylation
AHNAK	Neuroblast differentiation-associated protein AHNAK	25	Altered compartmentalization and molecular interactions; modulates stem cell differentiation [47–50]
ANXA2	Annexin A2; Putative annexin A2-like protein	1	Effect on chemosensitivity, possibly also AML prognosis [51–53]
APOBR	Apolipoprotein B receptor	3	-
<u>DBN1</u>	Drebrin	1	Actin organization, Mg ²⁺ transport [54–56]
<u>DUT</u>	Deoxyuridine 5'-triphosphate nucleotidohydrolase, mitochondrial	1	Possibly no effect on the enzymatic activity [57]
<u>GP1BB</u>	Platelet glycoprotein Ib beta chain	1	-
ITPR1	Inositol 1,4,5-trisphosphate receptor type 1	1	Cellular calcium homeostasis [58,59]
KCTD12	BTB/POZ domain-containing protein KCTD12	1	Cell cycle regulation; cancer support [60]
<u>MSL1</u>	Male-specific lethal 1 homolog	1	Epigenetic regulation in cancer [61]
PBXIP1	Pre-B-cell leukemia transcription factor-interacting protein 1	1	-
PLEC	Plectin	7	Mitosis/centrosome localization [62]
PRKCD	Protein kinase C delta type	2	Phosphorylation profile is important for molecular interactions [63–65]
<u>RCOR3</u>	REST corepressor 3	3	-
<u>SMC4</u>	Structural maintenance of chromosomes protein 4	1	Multisite mitosis-associated phosphorylation [66–69]
<u>STMN1</u>	Stathmin	2	Cancer chemoresistance and progression, stemness marker, and PI3K target. Possibly an adverse prognostic impact in hematological malignancies, including AML [70–74]
<u>TOP2A</u>	DNA topoisomerase 2-alpha	2	Regulation of S phase entry, targeted by etoposide and mitoxantrone [75,76]

Based on the data presented in Table 2 and Tables S10 and S11, the following main observations were made:

- Three of these 16 proteins are regarded as markers of neutrophil differentiation (ANXA2, ITPR1, and PRKCD; see Figure 3).

- For seven of these sixteen proteins, differences were detected for at least two phosphosites, i.e., the phosphorylation profile differed and not only in the phosphorylation of a single site.
- For certain proteins, opposite differences/effects on various phosphosites were observed, i.e., AHNAK, PLEC, and TOP2A (see Table S10).
- For other proteins, the total protein level was increased/decreased in one direction between the two patient subsets, whereas the level of (certain) phosphorylations was altered in an opposite direction (AHNAK, ITPR, PBXIP1, PLEC, TOP2A); these observations show that altered phosphorylation reflects the altered regulation of phosphorylation and not the difference in total protein level.
- Some of these phosphosites seem important for molecular compartmentalization (AHNAK) or molecular interactions/intracellular signaling (AHNAK, ANXA2, GP1BB, ITPR1, PLEC, PRKCD, STMN1).
- The phosphorylation status also seems important for the regulation of fundamental cellular processes, especially cell cycle regulation/cell growth (ANXA2, KCTD12, PLEC, PRKCD, SMC4, TOP2A) but also stemness/stem cell differentiation (AHNAK, STMN1), survival/chemosensitivity (ANXA2, DUT, PRKCD, TOP2A), cytoskeleton functions (DBN1, PLEC), electrolyte balance/transport (DBN1, ITPR1), nucleotide metabolism (DUT), cell migration (AHNAK), nutrition (APOBR), and epigenetic/transcriptional regulation (MSL1, PBXIP1, RCOR3, TOP2A).
- Some of the proteins seem to be implicated in carcinogenesis (KCTD12, MSL1, PBXIP1, PRKCD, STMN1) and even AML chemosensitivity (ANXA2, STMN1, TOP2A).

To conclude, primary AML cells and normal CD34⁺ bone marrow cells show complex differences in their proteomic profiles, and this complexity is further increased by additional variations between patient subsets with regard to post-translational modulation/phosphorylation for 16 of the 121 differentially abundant proteins.

3.7. Variation of the Biological Context of Transferrin and Transferrin Receptors That Are Both Differentially Abundant When Comparing Normal and Leukemic Hematopoietic Cells; Identification of a Patient Minority Whose AML Cells Show Similarities with Normal Cells in Regulation of Cellular Iron Uptake

Our statistical comparison of primary AML cells and normal CD34⁺ bone marrow cells showed that both transferrin and the transferrin receptor were differentially abundant with low levels in the leukemic cells; transferrin was then the protein with the lowest *p*-value and its receptor also showed a highly significant decrease (Figure 4, Table S2). Transferrin and its receptor constitute the main mechanism for the cellular uptake of iron [77–79]. Furthermore, iron metabolism and the regulation of iron-dependent ferroptosis seem to have a prognostic impact on human AML [80–88]. For these reasons, we compared iron metabolism in AML cells and normal CD34⁺ bone marrow cells in more detail.

The Reactome term “Iron metabolism” and the KEGG term “Ferroptosis” included only three of the 121 differentially abundant proteins showing at least a 2-fold difference when comparing AML cells and normal CD34⁺ bone marrow cells and, in addition, being identified in the z-score analysis (Tables S1, S2 and S5). However, 13 additional iron metabolism/ferroptosis proteins also showed statistically significant (Welch’s *t*-test with Benjamini–Hochberg correction) but without being identified in the z-score analysis (see figure legend). Our comparison of iron metabolism/ferroptosis regulation in primary AML cells and normal CD34⁺ bone marrow cells was, therefore, based on these 16 proteins (Table S12). The identified proteins are involved in the regulation of cellular iron uptake and intracellular endosomal release (TFRC, TF, ACO1, several V-ATPase components), regulation of iron homeostasis (ACO1), and/or various steps/characteristics of ferroptosis—i.e., altered regulation of cellular iron metabolism/handling (TFR, TFRC, ACO1, CUL1,

CAND1), altered redox balance (GLRX3), altered lipid metabolism (ACSL1), and protein ubiquitination/degradation (RPS27A, CAND1, CUL1, NED8, ATG7) (Table S12, [80–94]).

We conducted an unsupervised hierarchical clustering analysis based on the 16 differentially abundant metabolic/ferroptotic proteins identified as described above (Figure 6). The proteins are listed to the left in the figure. Only three proteins, TF, TFRC (both increased in normal cells), and ATP6V0D1 (higher in AML cells), showed ≥ 2 -fold differences when comparing leukemic and normal cells, whereas the other 13 differentially abundant proteins showed < 2 -fold differences that still reached statistical significance ($p < 0.05$) when comparing the two complete groups. It can be seen that the left main cluster included a majority of 40 AML patients (indicated by blue color), whereas the right minor main cluster had one right subcluster that included the eight normal CD34⁺ cell populations (indicated by corn silk color at the top of the figure) and another subcluster that included 10 AML patients (blue color).

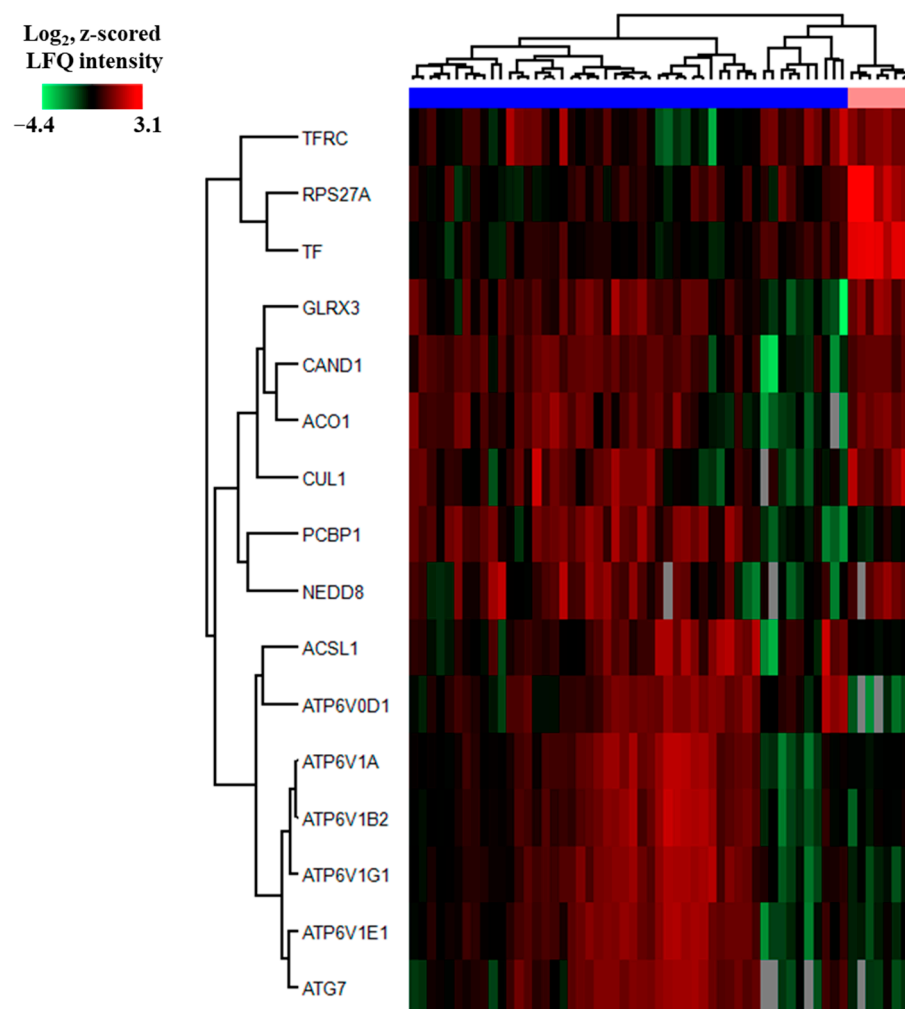


Figure 6. Hierarchical clustering analysis based on the 16 metabolic/ferroptotic proteomic profiles for primary AML cells derived from 50 patients and eight CD34⁺ bone marrow cell populations derived from healthy individuals (HI). This analysis is based on the expression of 16 proteins (i) that were abundant in at least 70% of the AML cell populations or normal CD34⁺ bone marrow populations, and (ii) differed significantly in the Welch's *t*-test with Benjamini–Hochberg correction when comparing leukemic and normal cells. The clustering of normal (corn silk color) and leukemic cells (blue color) is shown at the top of the figure. The ranking of patients from left to right is shown at the top of the figure and is also presented in Table S13. All proteins included in the analysis are known regulators of iron metabolism/ferroptosis according to the Reactome/KEGG classifications.

They included (i) three proteins showing significance after the Z-statistics analysis (TF, TFRC, ATP6V0D1); (ii) five proteins showing significance in the Welch's *t*-test with Benjamini–Hochberg correction and, in addition, a fold change corresponding to >2.0 (ACO1, ACSL1, ATP6V1G1, ATP6V1E1, ATG7); and (iii) eight proteins showing significance in the Welch's *t*-test with Benjamini–Hochberg correction but having a lower fold change (RPS27A, GLRX3, CAND1, CUL1, PCBP1, NEDD8, ATP6V1A, ATP6V1B2).

It can be seen from Figure 6 that the minority of 10 patients clustering together with the normal CD34⁺ bone marrow cells differed in their proteomic profile both from the normal cells (although the common clustering reflects certain similarities) and from the 40 other AML cell populations. Thus, we identified a minority of 10 AML patients whose leukemic cells showed a different iron metabolism/ferroptosis protein profile compared with cells derived from the other 40 patients and from the eight normal individuals. The similarities between the 10 exceptional AML patients and the healthy individuals especially included the absorption pair transferrin/transferrin receptor and V-ATPase components that are important for vacuolar acidification and thereby intracellular iron release [77–79].

We compared the clinical and biological characteristics of this minority of 10 AML patients (i.e., the right AML subcluster) with the other 40 patients (the left main cluster). First, all 10 of the exceptional patients had high-risk/chemoresistant AML (i.e., primary resistance or death from later resistant relapse), whereas 18 of the 40 other patients reached long-term AML-free survival (Fisher's exact test, $p = 0.0085$). Second, the minority of 10 patients (median age 62 years; range 29–80 years; IQR 67.25 – 57.50 = 9.75) had a higher age than the 40 patients in the left main cluster (median 46 years; range 18–67 years; IQR 57.00 – 37.25 = 19.75; Mann–Whitney U-test, $p = 0.00214$). Finally, the 10 AML patients in the right main cluster and the 40 other patients in the left main cluster did not differ significantly with regard to:

- Male versus female ratio.
- A low frequency of secondary AML.
- Morphological signs of differentiation, i.e., frequency of monocytic FAB-M4/M5 AML variants (Fisher's exact test, $p = 0.1548$).
- Number of patients with at least 20% AML cells expressing the CD34 stem cell marker ($p = 0.0706$).
- Even though all six patients with the favorable inv(16) karyotype were localized in various subclusters among the left 40 patients, this difference did not reach statistical significance.
- Other cytogenetic abnormalities did not differ significantly between the two main AML patient subsets; both subsets showed heterogeneity with regard to karyotype.
- The frequencies of *FLT3-ITD* or *NPM1-INS* did not differ.
- Both groups were heterogeneous with regard to the ELN risk classification by genetics at the time of initial diagnosis [2] (see Tables 1 and S13). The minority of 10 patients in the right main cluster included three patients with ELN adverse prognosis, four patients with intermediate/adverse prognosis, and one patient for each of the three groups: favorable, intermediate, and unclassified.
- The peripheral blood blast count of the 10 patients that were clustered together with normal CD34⁺ cells (median $26.0 \times 10^9/L$, range $5\text{--}71 \times 10^9/L$, IQR $49.75 - 9.75 = 40.0 \times 10^9/L$) did not differ significantly from the other 40 AML patients (median $33.5 \times 10^9/L$, range $4.0\text{--}351 \times 10^9/L$, IQR $99.5 - 27.5 = 72.0 \times 10^9/L$). Similarly, the percent AML blasts in the bone marrow did not differ between the minor subset of 10 patients (median 63.5%, range 25–99%, IQR $95.00 - 49.25 = 45.75\%$) and the majority of 40 patients (median 83.5%, range 25–99%, IQR $86 - 53 = 33$) in the other

main cluster. These observations suggest that there is no major difference between the two patient subsets with regard to AML cell burden.

- All 10 patients clustering together with the normal CD34⁺ cells belonged to the left 22-patient cluster/subset identified in Figure 5 (see Table S8). Thus, in the 121-protein clustering a subset of 22 patients was identified that showed few signs of differentiation and adverse prognosis (i.e., decreased frequency of long-term survival), and in this second clustering analysis (Figure 6) based on regulators of iron metabolism/ferroptosis, a subset among these 22 patients (i.e., patients with fewer signs of differentiation) was identified with a particularly high-risk disease/adverse prognosis.

To summarize, our iron metabolic/ferroptotic clustering analysis based on these 16 differentially abundant proteins identified a heterogeneous minority of elderly patients with chemoresistant AML; these patients were heterogeneous both with regard to AML cell differentiation, CD34 expression, karyotype, *FLT3-ITD*, and *NPM1-INS*. Thus, the significant difference in long-term AML-free survival between these two patient subsets cannot be explained by different frequencies of other prognostic parameters.

4. Discussion

We compared the proteomic profiles for primary human AML cells and normal CD34⁺ bone marrow cells. Even though the two groups differed with regard to the expression of several neutrophil markers and regulators of iron metabolism/ferroptosis, the patients were heterogeneous even with regard to the expression of these markers.

4.1. Methodological Considerations

Our study included 50 consecutive patients receiving intensive AML therapy; they came from a defined geographical area during a defined time period [24]. Our study should, therefore, be regarded as a population-based study of AML patients with a high percentage of AML cells among circulating leukocytes. The morphological classification of differentiation was performed according to the FAB/WHO 2016 classification that represents a standardized system describing detailed and updated morphological/biological/diagnostic criteria for the subset “AML not otherwise specified”, including how various subsets in this class correspond to the previous FAB classification [95].

We also classified our patients according to the ELN risk classification by genetics at initial diagnosis (Table 1). Because the genetic analyses were incomplete for several early patients and additional biological material was not available, twelve patients were classified as intermediate/adverse and six patients could not be classified. We would expect most of the intermediate/adverse patients to have an intermediate risk [2].

Our study did not include patients with the uncommon erythroid (FAB-M6) and megakaryocytic (FAB-M7) variants [1,95]. The higher levels of platelet/megakaryocyte markers in the normal CD34⁺ cells probably reflect the heterogeneity of CD34⁺ cells including immature erythroid/megakaryocytic stages [11,13–15,96].

The use of gradient-separated AML cells from peripheral blood in our study has been discussed in detail in a previous study. The reasons for this methodological approach and its possible limitations are as follows [24]:

- As discussed in previous methodological publications, more extensive cell separation procedures can alter the functional characteristics of AML cells [97,98]; by selecting patients with a high percentage of circulating AML blasts, we could prepare highly enriched AML cell populations by using simple gradient separation alone. This would not be possible with relatively low but still diagnostic percentages of bone marrow blasts.

- A previous methodological study showed that cryopreservation had only a limited influence on the proteomic profiles of AML cells [34].
- The AML cell population has a hierarchical organization, and leukemic stem cells are possibly responsible for how mortality relates to AML chemoresistance [98], but despite this, we investigated the whole AML cell population. However, several previous studies have also demonstrated that biological characteristics of the whole AML cell population reflect the risk of resistance after chemotherapy, e.g., cytokine release, gene expression, and epigenetic and pathway activation profiles (for reference, see ref. [24]).
- Previous studies have shown that AML patients with and without peripheral blood leukemization have comparable frequencies of various genetic abnormalities [99], i.e., there is no strong enrichment of certain (high-risk) abnormalities when using our strategy for inclusion of patients.
- Previous studies suggest that leukemization may have an adverse prognostic impact, and if so, our inclusion of only patients with leukemization may cause an enrichment of patients with a more aggressive disease compared with AML in general. However, studies of the possible independent prognostic impact of high peripheral blood AML blast counts have given conflicting results [100,101]; if an effect is present, it must be weak [102] and/or may be present only for certain minor patient subsets [100] and/or be present only when counts exceed $50\text{--}100 \times 10^9/\text{L}$ [100,103,104] (most of our patients had lower counts).
- Finally, all our patients had >20% blasts in the bone marrow, whereas certain forms of AML can now be diagnosed by lower blast percentages in bone marrow or peripheral blood [1].

Even though it can be argued that our observations are relevant for AML in general, our results should be interpreted with great care, and, due to our selection of patients with leukemization, they may be representative only for patients with >20% blasts in the bone marrow and/or peripheral blood leukemization.

4.2. Increased Neutrophil Differentiation of Primary AML Ells Compared with Normal CD34⁺ Bone Marrow Cells

We identified 121 differentially abundant proteins that should be regarded as markers of neutrophil differentiation (Figure 2A Reactome terms, Tables S1–S4). However, the low number of proteins included, the lower statistical significance of other GO/Reactome/KEGG terms (Figure 2A), the results from the volcano plot analysis (Figure 2B), and the relatively few and small identified protein interaction networks (Figure 4) possibly reflect a biological heterogeneity of those differentially abundant proteins not associated with neutrophil differentiation. However, the differentially abundant proteins included cross-communicating cell surface molecules and their downstream mediators:

- *TLR2 and TLR2 signaling in AML.* Primary AML cells express functional TLRs, including TLR2 and TLR4 [105]. Both of these receptors can bind endogenous agonists [106], although these observations have been questioned and may at least partly be due to a function as assistants due to their binding of other ligands [107]. The transmembrane TLR2 protein was increased in our AML cells (Figure 2). The downstream TLR2 signaling includes MYD88, various IRAKs, TAK1, TAB1/2, and TRF6 adaptor molecules; IRAK-6 thus seems responsible for recruitment to the receptor complex that moves to the cytoplasm and activates NFκB and the AP-1 transcription factor [108]. This MYD88-dependent downstream signaling is not specific for TLR2 but seems common for various TLRs, including TLR4.

- *Alternative signaling downstream to TLR2.* Alternative TLR2/MyD88 downstream targets are PI3K-Akt with the enhancement of ERK1/2, p38 MAPK, JNK1/2, and focal adhesion kinase (FAK) activation/phosphorylation [106]. Many of these targets are also important for the downstream signaling of TLR4 [108], a receptor that interacts with S100A9 (see below) and thereby regulates AML cell differentiation by targeting p38 and ERK1/2 [109,110]. Thus, there are functional links between TLR2, TLR4, and S100A9/S100A10.
- *Integrins and integrin signaling including RHO GTPases.* Our study suggests that the integrin expression profile is altered in AML cells, especially ITGAX, ITGAL, and ITGA2B (Figure 2, Table S7). Integrins bind a wide range of cell adhesion and extracellular matrix molecules, and their outside-in signaling modulates the activation of several intracellular mediators including FAK, PI3K, AKT, mTOR, ERK, and JNK [111–114] as well as RHO-GTPases that are also involved in inside-out signaling and the regulation of the proliferation, differentiation and possibly chemosensitivity of malignant cells, including AML cells [111,115–120]. Thus, integrins share downstream target TLR2 and/or S100 proteins (see below).
- *S100 proteins in AML.* Our results suggest that S100A8/9/11, especially, shows increased levels in primary AML cells. Both S100A8 and S100A9 are regarded as differentiation markers in AML but also seem to limit/inhibit further AML cell differentiation [121]. A high mRNA expression of S100A8 is associated with adverse prognosis in AML with a normal karyotype, and this prognostic impact may depend on its effects on autophagy, the production of reactive oxygen species, and the mitochondrial regulation of apoptosis [121,122]. Furthermore, S100A8 and S100A9 exist both as homodimers and heterodimers, and the effect of the heterodimer is difficult to predict. Thus, there is a crosstalk both between S100A8 and S100A9 [121] and also between S100A8 and TLR4 [109]. Finally, S100A11 is also a regulator of cellular proliferation and seems to have a prognostic impact on certain malignancies, but this is the first report to suggest a role in human AML [123].
- *Fibrinogen.* Fibrinogen is a hexameric glycoprotein that consists of two sets of three α , β , or γ chains [124]; it is mainly synthesized in hepatocytes but can also be abundant in certain other cells [125]. The expression of all the fibrinogen α , β , and γ chains was generally higher for normal CD34⁺ bone marrow cells than AML cells (Figure 2, Table S4). Fibrinogen can bind to α M β 2 and α X β 2 integrins [126] as well as soluble ferritin [127], whose systemic levels can be increased and predict adverse prognosis in AML [128]. These observations further support our hypothesis that AML cells and normal CD34⁺ bone marrow cells differ with regard to integrin function but also iron metabolism (Figure 4) due to an increased expression of transferrin–transferrin receptors in CD34⁺ cells.

Taken together, these observations suggest that the differentially abundant proteins (Tables S5–S7) include TLR2 and several integrins together with certain common and interacting downstream mediators. Several of the proteins are regarded as potential therapeutic targets in AML, including the integrin system [116,117,129] with the downstream MAP kinases [130–136], S100A molecules [121,122,137,138], and TLR2/4 with their downstream mediators [106,108], including the RHO GTPases [111,115–120,139,140]. Finally, aldehyde dehydrogenase is also regarded as a possible therapeutic target in AML [141–144], and the biological context of this enzyme seemed to differ between AML cells and normal CD34⁺ cells.

Future studies have to clarify whether the high levels of possible therapeutic targets in our present study represent a high dependency on these mediators and, thereby, susceptibility to targeted therapy, or whether resistance to targeting due to the high levels requires

high inhibitor concentrations for antileukemic efficiency. Furthermore, the therapeutic targeting of these differentially abundant mediators would probably also influence the function of various immunocompetent cells known to infiltrate the leukemic bone marrow microenvironment [145,146]; they may thereby influence the balance between antileukemic and AML-supporting immune activity. Thus, the therapeutic targeting of these mechanisms may have direct effects on AML cells and additional indirect effects via neighboring immunocompetent or bone marrow mesenchymal/stromal cells [108].

Previous studies have investigated the possible prognostic impact of differentiation markers in AML, including CD34 expression and Sudan black staining; these early studies suggested that such markers had no/uncertain prognostic impact [147,148], whereas certain recent studies suggest that CD34 expression is important in certain AML subsets [149,150]. Furthermore, minimal residual disease has now become important for clinical prognostication in AML [151–153], and the pretreatment burden of immature/undifferentiated cells (i.e., the degree of differentiation within the AML cell population) can be combined with MRD evaluation to improve prognostication [154]. In this context, we conclude/suggest that the evaluation of AML cell differentiation with proteomic profiling rather than the use of single or a limited number of differentiation markers, and possibly in combination with MRD estimation, should be regarded as a possible strategy for prognostication in AML. Future clinical studies then have to clarify whether other patients with a similar differentiation marker profile as described for patients with a favorable karyotype in our present study (Figure 3, right patient subset; see also Table S8) also have a similar favorable prognosis.

We identified 121 proteins that showed differential expression when comparing all 50 primary AML cell populations with the normal CD34⁺ bone marrow stem/progenitor cells. However, even the expression of these differentially abundant proteins showed a considerable variation between individual patients with regard to protein levels, and these markers could therefore be used for further subclassification of our 50 patients into two main subsets (see Figure 5). Furthermore, our phosphoproteomic studies illustrate that the proteomic complexity is further increased by differences in the degree of post-translational phosphorylation between the two main patient subsets for 16 of the 121 differentially abundant proteins (see Section 3.6). Previous studies suggest that these phosphoproteomic differences (see Tables 2, S10 and S11) are functionally important, although it should be emphasized that most of these functional studies have not been performed in normal or malignant hematopoietic cells [94,106–136].

We conducted a clustering analysis based on the 121 proteins, showing at least a two-fold difference when comparing AML cells and CD34⁺ bone marrow cells (Table S5), and this analysis identified a subset of 28 patients characterized by neutrophil differentiation and favorable prognosis (Table S7 for details). These 28 patients were also characterized by higher peripheral blood blast counts than the other patients, whereas the bone marrow blast percentages did not differ. These observations are consistent with the hypothesis that the degree of peripheral blood leukemization is mainly determined by the biological characteristics of the AML cells rather than the AML cell burden. Furthermore, this hypothesis is further supported by the previous observation that hyperleukocytosis is also more common in patients with myelomonocytic AML cells [155,156]. Finally, it is not unexpected that AML cells sharing biological characteristics with a mature normal myeloid cell type that is determined to enter the circulation also show a similar and higher degree of migration/leukemization compared with more undifferentiated ML cells.

4.3. Iron Metabolism and Regulation of Ferroptosis in Primary AML Cells; Comparison with Normal CD34⁺ Bone Marrow Cells and the Variation Between Patients

Ferroptosis is a form of programmed cell death characterized by altered iron metabolism together with the formation of reactive oxygen species and altered lipid

metabolism; it should thus be regarded as iron-dependent cell death [80–88]. We observed several differences between AML cells and normal CD34⁺ bone marrow cells with regard to iron uptake. First, decreased AML cell levels of the transferrin receptor suggest decreased uptake of iron-containing transferrin, and decreased receptor-mediated transferrin uptake is possibly reflected by the decreased AML cell transferrin levels. Second, V-ATPase is important for endosomal acidification, which is essential for intracellular iron release after endosomal uptake both in the cytoplasm and possibly also in mitochondria [79]. In our clustering analysis based on the 16 differentially abundant proteins involved in iron metabolism/ferroptosis (Figure 4), we identified a patient subset characterized by adverse prognosis (i.e., primary chemoresistance or later relapse) that clustered together with the normal CD34⁺ cells and showed relatively low levels of most iron metabolism/ferroptosis proteins. These observations are also consistent with a previous study describing increased mRNA levels of V-ATPase components and different iron metabolism for primary AML cells derived from patients with favorable prognosis [157], as well as another study describing an association between increased relapse risk and decreased protein levels of V-ATPase components [24]. Finally, in contrast to the patients identified based on the clustering analysis of all highly differing proteins (i.e., more than 2-fold and including several differentiation markers; see Figure 2), the patient subsets with adverse prognosis identified in the clustering analysis of iron/ferroptosis markers (Figure 3) did not differ from the other patients with regard to age, morphological AML cell differentiation, AML cell expression of the CD34 stem cell marker, or genetic abnormalities. Taken together, these observations suggest that the regulation of iron metabolism/ferroptosis should be further investigated as a possible independent prognostic marker for AML patients receiving intensive conventional therapy.

4.4. Limitations of This Present Study

The complexity of cellular proteins far exceeds that of the approximately 20,000 protein-encoding genes in humans [158]. The term proteoform is therefore used to describe the complexity of the protein system [158–160], and it is defined as all the different molecular forms in which the protein product of a single gene can be found [159]. This variation is created by several mechanisms and includes (i) the protein-encoding gene and its genetic variants, (ii) the various alternatives for RNA splicing, and (iii) variations in folding/function compared with the canonical protein due to genetics/amino acid sequence differences, splice variants, posttranslational modification (e.g., phosphorylation, methylation, acetylation, glycosylation, lipidation), and protein truncation (e.g., activation by proteolytic cleavage) [158–165]. Our present study has only investigated a part of this complexity, i.e., an estimate of the total protein level and for the differentiation studies of posttranslational phosphorylation. We did not, for example, investigate splicing variants (also referred to as isoforms in the previous literature and the gene database) that are important for the function of the iron metabolism/ferroptosis regulators examined in our present study (Figure 4) [165]. Many of these proteins are abundant as various proteoforms; this is exemplified by the proteins listed in Table S11. Future studies, therefore, have to address the limitations of our present study and (i) investigate the complexity of AML also in the uncommon erythroid, megakaryocytic, and myelofibrotic AML variants that were not present among our patients (see Table 1), as well as (ii) additional post-translational modulations and/or the presence of various proteoforms that may differ between leukemic and normal CD34⁺ cell and/or between AML patient subsets. Finally, our study included relatively few patients and our observations therefore need to be verified in larger prospective clinical studies.

Our studies on iron metabolism/ferroptosis show a significantly increased risk of relapse/resistance for a relatively small subset of AML patients having similarities in cellular iron metabolism when compared with normal CD34⁺ bone marrow cells. The patients within this subset are heterogeneous with regard to ELN genetic risk classification [2] but the number of patients in our study is too low to allow for a reliable additional biological characterization of the patients included in this minor subset.

As discussed in Section 4.1, our present observations may be relevant only for AML patients with relatively high levels of AML blasts in bone marrow and peripheral blood.

5. Summarizing Conclusions

We compared the proteomic profiles of pretreatment AML (a bone marrow malignancy) cells derived at the first time of diagnosis with a normal counterpart, i.e., normal CD34⁺ bone marrow cells. Based on differentially abundant cellular proteins, we identified three patient subsets that only partially reflected the AML-associated genetic abnormalities. (i) One subset was identified based on the expression of neutrophil differentiation markers and included patients with favorable karyotypes. (ii) Among the other patients without extensive differentiation, we identified a subset with a particularly adverse prognosis and an AML cell profile of iron metabolism/ferroptosis regulators showing similarities with the normal CD34⁺ cells. (iii) The remaining subset showed few signs of differentiation but an altered expression of iron metabolism/ferroptosis regulators.

Supplementary Materials: The following supporting information can be downloaded at: <https://www.mdpi.com/article/10.3390/proteomes13010011/s1>, Table S1: Proteins showing increased levels in primary AML cells compared with normal CD34⁺ bone marrow cell; Table S2: Proteins showing increased levels in normal CD34⁺ bone marrow cells compared with primary AML cell; Table S3: Reactome classification of differentially abundant proteins when comparing 50 primary AML cell populations and CD34⁺ bone marrow cells derived from eight healthy individuals, an overview of proteins showing at least a median 2-fold increase in primary AML cells; Table S4: Differential expression of protein when comparing 50 primary AML cell populations and CD34⁺ bone marrow cells derived from eight healthy individuals, an overview of proteins showing at least a median 2-fold increase in normal CD34⁺ cells compared with AML cells; Table S5: Proteins showing a differential expression when comparing AML cells derived from 50 patients and normal CD34⁺ bone marrow cells derived from eight healthy individuals; an overview of identified proteins after analysis based on Welch's *t*-test with Benjamini correction and fold change significance (z-score test); Table S6: Proteins showing differential expression when comparing AML cells derived from 50 patients and normal CD34⁺ bone marrow cells derived from eight healthy individuals; an overview of identified proteins after analysis based on Welch's *t*-test with Benjamini correction and fold change significance (z-score test); Table S7: Hierarchical clustering analysis of 121 differentially abundant proteins when comparing AML cells and normal CD34⁺ bone marrow cells; the protein subclassification into two main clusters as shown in Figure 5; Table S8: Clinical and biological characteristics of the 50 AML patients included in the study. Patients are listed according to the clustering analysis presented in Figure 5 (listed from left to right, see the top of the figure) in the article, i.e., the upper part of the table represents the left 22 patients in the cluster analysis and the lower part the right subset of 28 patients; Table S9: Clinical and biological characteristics of 50 AML patients included in the study; a comparison of two patient subsets identified by unsupervised hierarchical clustering analysis (Figure 5). Table S10: Protein phosphorylation of primary human AML cells, the identification of protein phosphorylation sites that (i) are localized on a subset (a total of 38 proteins) of the 121 proteins that showed differential expression (i.e., at least 2-fold difference) when comparing primary AML cells and normal CD34⁺ bone marrow cells; and (ii) in addition a statistically significant difference when each identified phosphosite was compared between the two patient subsets identified in the unsupervised hierarchical clustering analysis presented in Figure 5 (i.e., 23/28 right versus 18/22 left patients); Table S11: Differentially abundant proteins showing additional differences in protein

phosphorylation; Table S12: Proteins involved in the regulation of iron homeostasis/metabolism and/or ferroptosis and showing differential expression when comparing primary AML cells and normal CD34⁺ bone marrow cells; Table S13: Clinical and biological characteristics of the 50 AML patients included in the study; patient subclassification in an unsupervised hierarchical clustering analysis based on 16 differentially abundant proteins involved in regulation of iron metabolism and/or ferroptosis (Figure 6) (listed from left to right, see the top of the figure).

Author Contributions: Conceptualization, F.S., E.A., Ø.B. and M.H.-V.; data curation, F.S., E.A., Ø.B. and M.H.-V.; formal analysis, F.S., E.A., H.R., Ø.B. and M.H.-V.; funding acquisition, Ø.B.; investigation, F.S., E.A. and M.H.-V.; methodology, F.S., E.A. and M.H.-V.; project administration, Ø.B.; resources, Ø.B.; software, F.S., E.A. and M.H.-V.; supervision, Ø.B.; validation, F.S., E.A., H.R. and M.H.-V.; visualization, Ø.B. and M.H.-V.; writing—original draft, Ø.B.; writing—review and editing, F.S., E.A., H.R., Ø.B. and M.H.-V. All authors have read and agreed to the published version of the manuscript.

Funding: This research was funded by Kreftforeningen, the Norwegian Cancer Society (grant no. 100933) and by the Research Council of Norway INFRASTRUKTUR-program (project no. 295910). The funders had no role in the design of the study; in the collection, analyses, or interpretation of data; in the writing of the manuscript; or in the decision to publish the results.

Institutional Review Board Statement: This project was approved by the Regional Ethics Committee REK Vest (University of Bergen), references 2017/305 (approved 7 April 2017) and 2015/1759 (approved 5 November 2015). All cells were collected after obtaining written informed consent, and this study was conducted in accordance with the Declaration of Helsinki.

Informed Consent Statement: Informed consent was obtained from all subjects involved in this study.

Data Availability Statement: All proteomic raw data and MaxQuant output files together with the phosphoproteomic raw data can be found in the ProteomeXchange consortium with the dataset identifiers PXD014997 and PXD058846.

Acknowledgments: Mass spectrometry-based proteomic acquisition was performed at the Proteomics Unit at the University of Bergen (PROBE). PROBE is a member of the National Network of Advanced Proteomics Infrastructure (NAPI), which is funded by the Research Council of Norway.

Conflicts of Interest: The authors declare no conflicts of interest.

References

- Arber, D.A.; Orazi, A.; Hasserjian, R.P.; Borowitz, M.J.; Calvo, K.R.; Kvasnicka, H.M.; Wang, S.A.; Bagg, A.; Barbui, T.; Branford, S.; et al. International Consensus Classification of Myeloid Neoplasms and Acute Leukemias: Integrating morphologic, clinical, and genomic data. *Blood* **2022**, *140*, 1200–1228. [[CrossRef](#)] [[PubMed](#)]
- Döhner, H.; Wei, A.H.; Appelbaum, F.R.; Craddock, C.; DiNardo, C.D.; Dombret, H.; Ebert, B.L.; Fenaux, P.; Godley, L.A.; Hasserjian, R.P.; et al. Diagnosis and management of AML in adults: 2022 recommendations from an international expert panel on behalf of the ELN. *Blood* **2022**, *140*, 1345–1377. [[CrossRef](#)]
- Lo, M.Y.; Tsai, X.C.; Lin, C.C.; Tien, F.M.; Kuo, Y.Y.; Lee, W.H.; Peng, Y.L.; Liu, M.C.; Tseng, M.H.; Hsu, C.A.; et al. Validation of the prognostic significance of the 2022 European LeukemiaNet risk stratification system in intensive chemotherapy treated aged 18 to 65 years patients with de novo acute myeloid leukemia. *Am. J. Hematol.* **2023**, *98*, 760–769. [[CrossRef](#)]
- Choi, J.H.; Shukla, M.; Abdul-Hay, M. Acute Myeloid Leukemia Treatment in the Elderly: A Comprehensive Review of the Present and Future. *Acta Haematol.* **2023**, *146*, 431–457. [[CrossRef](#)] [[PubMed](#)]
- Russo, D.; Povereli, N.; Bernardi, S.; Santarone, S.; Farina, M.; Borlenghi, E.; Onida, F.; Castagna, L.; Bramanti, S.; Carella, A.M.; et al. Venetoclax plus decitabine as a bridge to allogeneic hematopoietic stem cell transplantation in older patients with acute myeloid leukemia (VEN-DEC GITMO): Final report of a multicenter single arm phase 2 trial. *Lancet Haematol.* **2024**, *11*, e830–e838. [[CrossRef](#)] [[PubMed](#)]
- Pratz, K.W.; Jonas, B.A.; Pullarkat, V.; Thirman, M.J.; Garcia, J.S.; Döhner, H.; Recher, C.; Fiedler, W.; Yamamoto, K.; Wang, J.; et al. Long-term follow-up of VIALE-A: Venetoclax and azacitidine in chemotherapy-ineligible untreated acute myeloid leukemia. *Am. J. Hematol.* **2024**, *99*, 615–624. [[CrossRef](#)]
- Kantarjian, H.; Kadia, T.; DiNardo, C.; Daver, N.; Borthakur, G.; Jabbour, E.; Garcia-Manero, G.; Konopleva, M.; Ravandi, F. Acute myeloid leukemia: Current progress and future directions. *Blood Cancer J.* **2021**, *11*, 41. [[CrossRef](#)]

8. Griffioen, M.S.; de Leeuw, D.C.; Janssen, J.J.W.M.; Smit, L. Targeting Acute Myeloid Leukemia with Venetoclax; Biomarkers for Sensitivity and Rationale for Venetoclax-Based Combination Therapies. *Cancers* **2022**, *14*, 3456. [[CrossRef](#)]
9. Bhansali, R.S.; Pratz, K.W.; Lai, C. Recent advances in targeted therapies in acute myeloid leukemia. *J. Hematol. Oncol.* **2023**, *16*, 29. [[CrossRef](#)]
10. Orfao, A.; Matarraz, S.; Pérez-Andrés, M.; Almeida, J.; Teodosio, C.; Berkowska, M.A.; van Dongen, J.J.M.; EuroFlow. Immunophenotypic dissection of normal hematopoiesis. *J. Immunol. Methods* **2019**, *475*, 112684. [[CrossRef](#)] [[PubMed](#)]
11. Sonoda, Y. Human CD34-negative hematopoietic stem cells: The current understanding of their biological nature. *Exp. Hematol.* **2021**, *96*, 13–26. [[CrossRef](#)] [[PubMed](#)]
12. Gangenahalli, G.U.; Singh, V.K.; Verma, Y.K.; Gupta, P.; Sharma, R.K.; Chandra, R.; Luthra, P.M. Hematopoietic stem cell antigen CD34: Role in adhesion or homing. *Stem Cells Dev.* **2006**, *15*, 305–313. [[CrossRef](#)] [[PubMed](#)]
13. Kreissig, S.; Windisch, R.; Wichmann, C. Deciphering Acute Myeloid Leukemia Associated Transcription Factors in Human Primary CD34+ Hematopoietic Stem/Progenitor Cells. *Cells* **2023**, *13*, 78. [[CrossRef](#)] [[PubMed](#)]
14. Zhai, P.F.; Wang, F.; Su, R.; Lin, H.S.; Jiang, C.L.; Yang, G.H.; Yu, J.; Zhang, J.W. The regulatory roles of microRNA-146b-5p and its target platelet-derived growth factor receptor α (PDGFRA) in erythropoiesis and megakaryocytopoiesis. *J. Biol. Chem.* **2014**, *289*, 22600–22613. [[CrossRef](#)] [[PubMed](#)]
15. Yurino, A.; Takenaka, K.; Yamauchi, T.; Nunomura, T.; Uehara, Y.; Jinnouchi, F.; Miyawaki, K.; Kikushige, Y.; Kato, K.; Miyamoto, T.; et al. Enhanced Reconstitution of Human Erythropoiesis and Thrombopoiesis in an Immunodeficient Mouse Model with Kit(Wv) Mutations. *Stem Cell Rep.* **2016**, *7*, 425–438. [[CrossRef](#)] [[PubMed](#)]
16. Leader, A.; Hofstetter, L.; Spectre, G. Challenges and Advances in Managing Thrombocytopenic Cancer Patients. *J. Clin. Med.* **2021**, *10*, 1169. [[CrossRef](#)]
17. Carson, J.L.; Stanworth, S.J.; Dennis, J.A.; Trivella, M.; Roubinian, N.; Fergusson, D.A.; Triulzi, D.; Dorée, C.; Hébert, P.C. Transfusion thresholds for guiding red blood cell transfusion. *Cochrane Database Syst. Rev.* **2021**, *12*, CD002042. [[PubMed](#)]
18. Carson, J.L.; Stanworth, S.J.; Guyatt, G.; Valentine, S.; Dennis, J.; Bakhtary, S.; Cohn, C.S.; Dubon, A.; Grossman, B.J.; Gupta, G.K.; et al. Red Blood Cell Transfusion: 2023 AABB International Guidelines. *JAMA* **2023**, *330*, 1892–1902. [[CrossRef](#)]
19. Peseski, A.M.; McClean, M.; Green, S.D.; Beeler, C.; König, H. Management of fever and neutropenia in the adult patient with acute myeloid leukemia. *Expert Rev. Anti Infect. Ther.* **2021**, *19*, 359–378. [[CrossRef](#)]
20. Maschmeyer, G.; Bullinger, L.; Garcia-Vidal, C.; Herbrecht, R.; Maertens, J.; Menna, P.; Pagano, L.; Thiebaut-Bertrand, A.; Calandra, T. Infectious complications of targeted drugs and biotherapies in acute leukemia. Clinical practice guidelines by the European Conference on Infections in Leukemia (ECIL), a joint venture of the European Group for Blood and Marrow Transplantation (EBMT), the European Organization for Research and Treatment of Cancer (EORTC), the International Immunocompromised Host Society (ICHHS) and the European Leukemia Net (ELN). *Leukemia* **2022**, *36*, 1215–1226. [[PubMed](#)]
21. Janssen, J.J.W.M.; Löwenberg, B.; Manz, M.; Biemond, B.J.; Westerweel, P.E.; Klein, S.K.; Fehr, M.; Sinnige, H.A.M.; Efthymiou, A.; Legdeur, M.C.J.C.; et al. Addition of the nuclear export inhibitor selinexor to standard intensive treatment for elderly patients with acute myeloid leukemia and high risk myelodysplastic syndrome. *Leukemia* **2022**, *36*, 2189–2195. [[CrossRef](#)]
22. Kuusanmäki, H.; Dufva, O.; Vähä-Koskela, M.; Leppä, A.M.; Huuhtanen, J.; Vänttinen, I.; Nygren, P.; Klievink, J.; Bouhhal, J.; Pölönen, P.; et al. Erythroid/megakaryocytic differentiation confers BCL-XL dependency and venetoclax resistance in acute myeloid leukemia. *Blood* **2023**, *141*, 1610–1625. [[CrossRef](#)] [[PubMed](#)]
23. Zhao, L.; Yang, J.; Chen, M.; Xiang, X.; Ma, H.; Niu, T.; Gong, Y.; Chen, X.; Liu, J.; Wu, Y. Myelomonocytic and monocytic acute myeloid leukemia demonstrate comparable poor outcomes with venetoclax-based treatment: A monocentric real-world study. *Ann. Hematol.* **2024**, *103*, 1197–1209. [[CrossRef](#)] [[PubMed](#)]
24. Aasebø, E.; Berven, F.S.; Bartaula-Brevik, S.; Stokowy, T.; Hovland, R.; Vaudel, M.; Døskeland, S.O.; McCormack, E.; Batth, T.S.; Olsen, J.V.; et al. Proteome and Phosphoproteome Changes Associated with Prognosis in Acute Myeloid Leukemia. *Cancers* **2020**, *12*, 709. [[CrossRef](#)] [[PubMed](#)]
25. Bruserud, Ø. Effect of dipyridamole, theophyllamine and verapamil on spontaneous in vitro proliferation of myelogenous leukaemia cells. *Acta Oncol.* **1992**, *31*, 53–58. [[CrossRef](#)] [[PubMed](#)]
26. Hernandez-Valladares, M.; Aasebø, E.; Selheim, F.; Berven, F.S.; Bruserud, Ø. Selecting Sample Preparation Workflows for Mass Spectrometry-Based Proteomic and Phosphoproteomic Analysis of Patient Samples with Acute Myeloid Leukemia. *Proteomes* **2016**, *4*, 24. [[CrossRef](#)]
27. Aasebø, E.; Vaudel, M.; Mjaavatten, O.; Gausdal, G.; Van der Burgh, A.; Gjertsen, B.T.; Døskeland, S.O.; Bruserud, O.; Berven, F.S.; Selheim, F. Performance of super-SILAC based quantitative proteomics for comparison of different acute myeloid leukemia (AML) cell lines. *Proteomics* **2014**, *14*, 1971–1976. [[CrossRef](#)]
28. Thingholm, T.E.; Jørgensen, T.J.; Jensen, O.N.; Larsen, M.R. Highly selective enrichment of phosphorylated peptides using titanium dioxide. *Nat. Protoc.* **2006**, *1*, 1929–1935. [[CrossRef](#)]
29. Thingholm, T.E.; Larsen, M.R. The Use of Titanium Dioxide for Selective Enrichment of Phosphorylated Peptides. *Methods Mol. Biol.* **2016**, *1355*, 135–146. [[PubMed](#)]

30. Thingholm, T.E.; Larsen, M.R. Phosphopeptide Enrichment by Immobilized Metal Affinity Chromatography. *Methods Mol. Biol.* **2016**, *1355*, 123–133.
31. Thingholm, T.E.; Jensen, O.N.; Robinson, P.J.; Larsen, M.R. SIMAC (sequential elution from IMAC), a phosphoproteomics strategy for the rapid separation of monophosphorylated from multiply phosphorylated peptides. *Mol. Cell. Proteom.* **2008**, *7*, 661–671. [[CrossRef](#)] [[PubMed](#)]
32. Wiśniewski, J.R.; Zougman, A.; Nagaraj, N.; Mann, M. Universal sample preparation method for proteome analysis. *Nat. Methods* **2009**, *6*, 359–362. [[CrossRef](#)] [[PubMed](#)]
33. Hernandez-Valladares, M.; Aasebø, E.; Mjaavatten, O.; Vaudel, M.; Bruserud, Ø.; Berven, F.; Selheim, F. Reliable FASP-based procedures for optimal quantitative proteomic and phosphoproteomic analysis on samples from acute myeloid leukemia patients. *Biol. Proced. Online* **2016**, *18*, 13. [[CrossRef](#)] [[PubMed](#)]
34. Aasebø, E.; Mjaavatten, O.; Vaudel, M.; Farag, Y.; Selheim, F.; Berven, F.; Bruserud, Ø.; Hernandez-Valladares, M. Freezing effects on the acute myeloid leukemia cell proteome and phosphoproteome revealed using optimal quantitative workflows. *J. Proteom.* **2016**, *145*, 214–225. [[CrossRef](#)] [[PubMed](#)]
35. Cox, J.; Hein, M.Y.; Lubner, C.A.; Paron, I.; Nagaraj, N.; Mann, M. Accurate proteome-wide label-free quantification by delayed normalization and maximal peptide ratio extraction, termed MaxLFQ. *Mol. Cell. Proteom.* **2014**, *13*, 2513–2526. [[CrossRef](#)] [[PubMed](#)]
36. Pei, S.; Pollyea, D.A.; Gustafson, A.; Stevens, B.M.; Minhajuddin, M.; Fu, R.; Riemondy, K.A.; Gillen, A.E.; Sheridan, R.M.; Kim, J.; et al. Monocytic Subclones Confer Resistance to Venetoclax-Based Therapy in Patients with Acute Myeloid Leukemia. *Cancer Discov.* **2020**, *10*, 536–551. [[CrossRef](#)] [[PubMed](#)]
37. Kuusanmäki, H.; Leppä, A.M.; Pölonen, P.; Kontro, M.; Dufva, O.; Deb, D.; Yadav, B.; Brück, O.; Kumar, A.; Everaus, H.; et al. Phenotype-based drug screening reveals association between venetoclax response and differentiation stage in acute myeloid leukemia. *Haematologica* **2020**, *105*, 708–720. [[CrossRef](#)] [[PubMed](#)]
38. Reikvam, H.; Hovland, R.; Forthun, R.B.; Erdal, S.; Gjertsen, B.T.; Fredly, H.; Bruserud, Ø. Disease-stabilizing treatment based on all-trans retinoic acid and valproic acid in acute myeloid leukemia—Identification of responders by gene expression profiling of pretreatment leukemic cells. *BMC Cancer* **2017**, *17*, 630. [[CrossRef](#)]
39. Tyanova, S.; Temu, T.; Sinitcyn, P.; Carlson, A.; Hein, M.Y.; Geiger, T.; Mann, M.; Cox, J. The Perseus computational platform for comprehensive analysis of (prote)omics data. *Nat. Methods* **2016**, *13*, 731–740. [[CrossRef](#)]
40. Arntzen, M.Ø.; Koehler, C.J.; Barsnes, H.; Berven, F.S.; Treumann, A.; Thiede, B. IsobariQ: Software for isobaric quantitative proteomics using IPPL, iTRAQ, and TMT. *J. Proteome Res.* **2011**, *10*, 913–920. [[CrossRef](#)]
41. Jassal, B.; Matthews, L.; Viteri, G.; Gong, C.; Lorente, P.; Fabregat, A.; Sidiropoulos, K.; Cook, J.; Gillespie, M.; Haw, R.; et al. The reactome pathway knowledgebase. *Nucleic Acids Res.* **2020**, *48*, D498–D503. [[CrossRef](#)]
42. Schölz, C.; Lyon, D.; Refsgaard, J.C.; Jensen, L.J.; Choudhary, C.; Weinert, B.T. Avoiding abundance bias in the functional annotation of post-translationally modified proteins. *Nat. Methods* **2015**, *12*, 1003–1004. [[CrossRef](#)]
43. Kanehisa, M.; Furumichi, M.; Sato, Y.; Kawashima, M.; Ishiguro-Watanabe, M. KEGG for taxonomy-based analysis of pathways and genomes. *Nucleic Acids Res.* **2023**, *51*, D587–D592. [[CrossRef](#)] [[PubMed](#)]
44. Xie, Z.; Bailey, A.; Kuleshov, M.V.; Clarke, D.J.B.; Evangelista, J.E.; Jenkins, S.L.; Lachmann, A.; Wojciechowicz, M.L.; Kropiwnicki, E.; Jagodnik, K.M.; et al. Gene Set Knowledge Discovery with Enrichr. *Curr. Protoc.* **2021**, *1*, e90. [[CrossRef](#)]
45. Shannon, P.; Markiel, A.; Ozier, O.; Baliga, N.S.; Wang, J.T.; Ramage, D.; Amin, N.; Schwikowski, B.; Ideker, T. Cytoscape: A software environment for integrated models of biomolecular interaction networks. *Genome Res.* **2003**, *13*, 2498–2504. [[CrossRef](#)] [[PubMed](#)]
46. Sasnoor, L.M.; Kale, V.P.; Limaye, L.S. Supplementation of conventional freezing medium with a combination of catalase and trehalose results in better protection of surface molecules and functionality of hematopoietic cells. *J. Hematother. Stem Cell Res.* **2003**, *12*, 553–564. [[CrossRef](#)] [[PubMed](#)]
47. Sussman, J.; Stokoe, D.; Ossina, N.; Shtivelman, E. Protein kinase B phosphorylates AHNAK and regulates its subcellular localization. *J. Cell Biol.* **2001**, *154*, 1019–1030. [[CrossRef](#)]
48. Pankonien, I.; Otto, A.; Dascal, N.; Morano, I.; Haase, H. Ahnak1 interaction is affected by phosphorylation of Ser-296 on Cavβ₂. *Biochem. Biophys. Res. Commun.* **2012**, *421*, 184–189. [[CrossRef](#)]
49. Shtivelman, E.; Bishop, J.M. The human gene AHNAK encodes a large phosphoprotein located primarily in the nucleus. *J. Cell Biol.* **1993**, *120*, 625–630. [[CrossRef](#)] [[PubMed](#)]
50. Billing, A.M.; Dib, S.S.; Bhagwat, A.M.; da Silva, I.T.; Drummond, R.D.; Hayat, S.; Al-Mismar, R.; Ben-Hamidane, H.; Goswami, N.; Engholm-Keller, K.; et al. A Systems-level Characterization of the Differentiation of Human Embryonic Stem Cells into Mesenchymal Stem Cells. *Mol. Cell. Proteom.* **2019**, *18*, 1950–1966. [[CrossRef](#)] [[PubMed](#)]
51. He, K.L.; Deora, A.B.; Xiong, H.; Ling, Q.; Weksler, B.B.; Niesvizky, R.; Hajjar, K.A. Endothelial cell annexin A2 regulates polyubiquitination and degradation of its binding partner S100A10/p11. *J. Biol. Chem.* **2008**, *283*, 19192–19200. [[CrossRef](#)] [[PubMed](#)]

52. Spijkers-Hagelstein, J.A.; Mimoso Pinhanços, S.; Schneider, P.; Pieters, R.; Stam, R.W. Src kinase-induced phosphorylation of annexin A2 mediates glucocorticoid resistance in MLL-rearranged infant acute lymphoblastic leukemia. *Leukemia* **2013**, *27*, 1063–1071. [[CrossRef](#)]
53. Niu, Y.; Yang, X.; Chen, Y.; Jin, X.; Xie, Y.; Tang, Y.; Li, L.; Liu, S.; Guo, Y.; Li, X.; et al. Distinct prognostic values of Annexin family members expression in acute myeloid leukemia. *Clin. Transl. Oncol.* **2019**, *21*, 1186–1196. [[CrossRef](#)] [[PubMed](#)]
54. Uddin, B.; Partscht, P.; Chen, N.P.; Neuner, A.; Weiß, M.; Hardt, R.; Jafarpour, A.; Heßling, B.; Ruppert, T.; Lorenz, H.; et al. The human phosphatase CDC14A modulates primary cilium length by regulating centrosomal actin nucleation. *EMBO Rep.* **2019**, *20*, e46544. [[CrossRef](#)] [[PubMed](#)]
55. Zhang, R.; Hu, M.; Liu, Y.; Li, W.; Xu, Z.; He, S.; Lu, Y.; Gong, Y.; Wang, X.; Hai, S.; et al. Integrative Omics Uncovers Low Tumorous Magnesium Content as A Driver Factor of Colorectal Cancer. *Genom. Proteom. Bioinform.* **2024**, *22*, qzae053. [[CrossRef](#)] [[PubMed](#)]
56. Dorskind, J.M.; Sudarsanam, S.; Hand, R.A.; Ziak, J.; Amoah-Dankwah, M.; Guzman-Clavel, L.; Soto-Vargas, J.L.; Kolodkin, A.L. Drebrin Regulates Collateral Axon Branching in Cortical Layer II/III Somatosensory Neurons. *J. Neurosci.* **2023**, *43*, 7745–7765. [[CrossRef](#)] [[PubMed](#)]
57. Ladner, R.D.; Carr, S.A.; Huddleston, M.J.; McNulty, D.E.; Caradonna, S.J. Identification of a consensus cyclin-dependent kinase phosphorylation site unique to the nuclear form of human deoxyuridine triphosphate nucleotidohydrolase. *J. Biol. Chem.* **1996**, *271*, 7752–7757. [[CrossRef](#)] [[PubMed](#)]
58. Yule, D.I.; Straub, S.V.; Bruce, J.I. Modulation of Ca²⁺ oscillations by phosphorylation of Ins(1,4,5)P₃ receptors. *Biochem. Soc. Trans.* **2003**, *31*, 954–957. [[CrossRef](#)] [[PubMed](#)]
59. Soghoian, D.; Jayaraman, V.; Silane, M.; Berenstein, A.; Jayaraman, T. Inositol 1,4,5-trisphosphate receptor phosphorylation in breast cancer. *Tumour Biol.* **2005**, *26*, 207–212. [[CrossRef](#)] [[PubMed](#)]
60. Zhong, Y.; Yang, J.; Xu, W.W.; Wang, Y.; Zheng, C.C.; Li, B.; He, Q.Y. KCTD12 promotes tumorigenesis by facilitating CDC25B/CDK1/Aurora A-dependent G2/M transition. *Oncogene* **2017**, *36*, 6177–6189. [[CrossRef](#)]
61. Wang, M.Y.; Qi, B.; Wang, F.; Lin, Z.R.; Li, M.Y.; Yin, W.J.; Zhu, Y.Y.; He, L.; Yu, Y.; Yang, F.; et al. PBK phosphorylates MSL1 to elicit epigenetic modulation of CD276 in nasopharyngeal carcinoma. *Oncogenesis* **2021**, *10*, 9. [[CrossRef](#)]
62. Niwa, T.; Saito, H.; Imajoh-ohmi, S.; Kaminishi, M.; Seto, Y.; Miki, Y.; Nakanishi, A. BRCA2 interacts with the cytoskeletal linker protein plectin to form a complex controlling centrosome localization. *Cancer Sci.* **2009**, *100*, 2115–2125. [[CrossRef](#)]
63. Kramer, M.H.; Zhang, Q.; Sprung, R.; Day, R.B.; Erdmann-Gilmore, P.; Li, Y.; Xu, Z.; Helton, N.M.; George, D.R.; Mi, Y.; et al. Proteomic and phosphoproteomic landscapes of acute myeloid leukemia. *Blood* **2022**, *140*, 1533–1548. [[CrossRef](#)]
64. Deng, Y.; Hou, Z.; Li, Y.; Yi, M.; Wu, Y.; Zheng, Y.; Yang, F.; Zhong, G.; Hao, Q.; Zhai, Z.; et al. Superbinder based phosphoproteomic landscape revealed PRKCD_pY313 mediates the activation of Src and p38 MAPK to promote TNBC progression. *Cell Commun. Signal.* **2024**, *22*, 115. [[CrossRef](#)]
65. Zhang, L.; Keane, M.P.; Zhu, L.X.; Sharma, S.; Rozengurt, E.; Strieter, R.M.; Dubinett, S.M.; Huang, M. Interleukin-7 and transforming growth factor-beta play counter-regulatory roles in protein kinase C-delta-dependent control of fibroblast collagen synthesis in pulmonary fibrosis. *J. Biol. Chem.* **2004**, *279*, 28315–28319. [[CrossRef](#)] [[PubMed](#)]
66. Sutani, T.; Yuasa, T.; Tomonaga, T.; Dohmae, N.; Takio, K.; Yanagida, M. Fission yeast condensin complex: Essential roles of non-SMC subunits for condensation and Cdc2 phosphorylation of Cut3/SMC4. *Genes Dev.* **1999**, *13*, 2271–2283. [[CrossRef](#)]
67. Thadani, R.; Kamenz, J.; Heeger, S.; Muñoz, S.; Uhlmann, F. Cell-Cycle Regulation of Dynamic Chromosome Association of the Condensin Complex. *Cell Rep.* **2018**, *23*, 2308–2317. [[CrossRef](#)] [[PubMed](#)]
68. Robellet, X.; Thattikota, Y.; Wang, F.; Wee, T.L.; Pascariu, M.; Shankar, S.; Bonneil, É.; Brown, C.M.; D’Amours, D. A high-sensitivity phospho-switch triggered by Cdk1 governs chromosome morphogenesis during cell division. *Genes Dev.* **2015**, *29*, 426–439. [[CrossRef](#)]
69. Kao, L.; Wang, Y.T.; Chen, Y.C.; Tseng, S.F.; Jhang, J.C.; Chen, Y.J.; Teng, S.C. Global analysis of cdc14 dephosphorylation sites reveals essential regulatory role in mitosis and cytokinesis. *Mol. Cell. Proteom.* **2014**, *13*, 594–605. [[CrossRef](#)] [[PubMed](#)]
70. Liao, L.; Zhang, Y.L.; Deng, L.; Chen, C.; Ma, X.Y.; Andriani, L.; Yang, S.Y.; Hu, S.Y.; Zhang, F.L.; Shao, Z.M.; et al. Protein Phosphatase 1 Subunit PPP1R14B Stabilizes STMN1 to Promote Progression and Paclitaxel Resistance in Triple-Negative Breast Cancer. *Cancer Res.* **2023**, *83*, 471–484. [[CrossRef](#)]
71. Kuang, X.Y.; Jiang, H.S.; Li, K.; Zheng, Y.Z.; Liu, Y.R.; Qiao, F.; Li, S.; Hu, X.; Shao, Z.M. The phosphorylation-specific association of STMN1 with GRP78 promotes breast cancer metastasis. *Cancer Lett.* **2016**, *377*, 87–96. [[CrossRef](#)]
72. Handa, T.; Yokobori, T.; Obayashi, S.; Fujii, T.; Shirabe, K.; Oyama, T. Association Between High Expression of Phosphorylated-STMN1 and Mesenchymal Marker Expression and Cancer Stemness in Breast Cancer. *Anticancer Res.* **2023**, *43*, 5341–5348. [[CrossRef](#)] [[PubMed](#)]
73. Alsagaby, S.A. Biological roles of THRAP3, STMN1 and GNA13 in human blood cancer cells. *3 Biotech* **2024**, *14*, 248. [[CrossRef](#)] [[PubMed](#)]
74. Machado-Neto, J.A.; de Melo Campos, P.; Favaro, P.; Lazarini, M.; Lorand-Metze, I.; Costa, F.F.; Olalla Saad, S.T.; Traina, F. Stathmin 1 is involved in the highly proliferative phenotype of high-risk myelodysplastic syndromes and acute leukemia cells. *Leuk. Res.* **2014**, *38*, 251–257. [[CrossRef](#)] [[PubMed](#)]

75. Tamaichi, H.; Sato, M.; Porter, A.C.; Shimizu, T.; Mizutani, S.; Takagi, M. Ataxia telangiectasia mutated-dependent regulation of topoisomerase II alpha expression and sensitivity to topoisomerase II inhibitor. *Cancer Sci.* **2013**, *104*, 178–184. [[CrossRef](#)]
76. Atwal, M.; Lishman, E.L.; Austin, C.A.; Cowell, I.G. Myeloperoxidase Enhances Etoposide and Mitoxantrone-Mediated DNA Damage: A Target for Myeloprotection in Cancer Chemotherapy. *Mol. Pharmacol.* **2017**, *91*, 49–57. [[CrossRef](#)] [[PubMed](#)]
77. Nakamura, T.; Naguro, I.; Ichijo, H. Iron homeostasis and iron-regulated ROS in cell death, senescence and human diseases. *Biochim. Biophys. Acta Gen. Subj.* **2019**, *1863*, 1398–1409. [[CrossRef](#)] [[PubMed](#)]
78. Milto, I.V.; Suhodolo, I.V.; Prokopieva, V.D.; Klimenteva, T.K. Molecular and Cellular Bases of Iron Metabolism in Humans. *Biochemistry* **2016**, *81*, 549–564. [[CrossRef](#)] [[PubMed](#)]
79. Galy, B.; Conrad, M.; Muckenthaler, M. Mechanisms controlling cellular and systemic iron homeostasis. *Nat. Rev. Mol. Cell Biol.* **2024**, *25*, 133–155. [[CrossRef](#)]
80. Zhang, H.; Sun, C.; Sun, Q.; Li, Y.; Zhou, C.; Sun, C. Susceptibility of acute myeloid leukemia cells to ferroptosis and evasion strategies. *Front. Mol. Biosci.* **2023**, *10*, 1275774. [[CrossRef](#)]
81. Chen, X.; Li, J.; Kang, R.; Klionsky, D.J.; Tang, D. Ferroptosis: Machinery and regulation. *Autophagy* **2021**, *17*, 2054–2081. [[CrossRef](#)] [[PubMed](#)]
82. Ma, Z.; Ye, W.; Huang, X.; Li, X.; Li, F.; Lin, X.; Hu, C.; Wang, J.; Jin, J.; Zhu, B.; et al. The ferroptosis landscape in acute myeloid leukemia. *Aging* **2023**, *15*, 13486–13503. [[CrossRef](#)]
83. Tang, X.; Wang, Y.; Zhu, Y.; Guo, Y.; Liu, B. Basic mechanisms and novel potential therapeutic targets for ferroptosis in acute myeloid leukemia. *Ann. Hematol.* **2023**, *102*, 1985–1999. [[CrossRef](#)] [[PubMed](#)]
84. Fu, D.; Zhang, B.; Wu, S.; Feng, J.; Jiang, H. Molecular subtyping of acute myeloid leukemia through ferroptosis signatures predicts prognosis and deciphers the immune microenvironment. *Front. Cell Dev. Biol.* **2023**, *11*, 1207642. [[CrossRef](#)] [[PubMed](#)]
85. Zhu, K.; Lang, Z.; Zhan, Y.; Tao, Q.; Yu, Z.; Chen, L.; Fan, C.; Jin, Y.; Yu, K.; Zhu, B.; et al. A novel 10-gene ferroptosis-related prognostic signature in acute myeloid leukemia. *Front. Oncol.* **2022**, *12*, 1023040. [[CrossRef](#)]
86. Wu, F.; Xu, G.; Li, G.; Yin, Z.; Shen, H.; Ye, K.; Zhu, Y.; Zhang, Q.; Ou, R.; Liu, S. A prognostic model based on prognosis-related ferroptosis genes for patients with acute myeloid leukemia. *Front. Mol. Biosci.* **2023**, *10*, 1281141. [[CrossRef](#)] [[PubMed](#)]
87. Song, Y.; Tian, S.; Zhang, P.; Zhang, N.; Shen, Y.; Deng, J. Construction and Validation of a Novel Ferroptosis-Related Prognostic Model for Acute Myeloid Leukemia. *Front. Genet.* **2022**, *12*, 708699. [[CrossRef](#)]
88. Hong, Y.; Liu, Q.; Xin, C.; Hu, H.; Zhuang, Z.; Ge, H.; Shen, Y.; Zhao, Y.; Zhou, Y.; Ye, B.; et al. Ferroptosis-Related Gene Signature for Prognosis Prediction in Acute Myeloid Leukemia and Potential Therapeutic Options. *Int. J. Gen. Med.* **2024**, *17*, 3837–3853. [[CrossRef](#)]
89. Berndt, C.; Lillig, C.H. Glutathione, Glutaredoxins, and Iron. *Antioxid. Redox Signal.* **2017**, *27*, 1235–1251. [[CrossRef](#)] [[PubMed](#)]
90. Daniel, T.; Faruq, H.M.; Laura Magdalena, J.; Manuela, G.; Christopher Horst, L. Role of GSH and Iron-Sulfur Glutaredoxins in Iron Metabolism-Review. *Molecules* **2020**, *25*, 3860. [[CrossRef](#)] [[PubMed](#)]
91. Yarosz, E.L.; Kumar, A.; Singer, J.D.; Chang, C.H. Cullin 3-Mediated Regulation of Intracellular Iron Homeostasis Promotes Thymic Invariant NKT Cell Maturation. *Immunohorizons* **2023**, *7*, 235–242. [[CrossRef](#)]
92. Iwai, K. Regulation of cellular iron metabolism: Iron-dependent degradation of IRP by SCF^{FBXL5} ubiquitin ligase. *Free Radic. Biol. Med.* **2019**, *133*, 64–68. [[CrossRef](#)] [[PubMed](#)]
93. Sufan, R.I.; Ohh, M. Role of the NEDD8 modification of Cul2 in the sequential activation of ECV complex. *Neoplasia* **2006**, *8*, 956–963. [[CrossRef](#)] [[PubMed](#)]
94. Rodríguez-Celma, J.; Chou, H.; Kobayashi, T.; Long, T.A.; Balk, J. Hemerythrin E3 Ubiquitin Ligases as Negative Regulators of Iron Homeostasis in Plants. *Front. Plant Sci.* **2019**, *10*, 98. [[CrossRef](#)] [[PubMed](#)]
95. Arber, D.A.; Brunning, R.D.; Orazi, A.; Porwit, A.; Peterson, L.C.; Thiele, J.; Le Beau, M.M.; Hasserjian, R.P. Acute myeloid leukemia, NOS. In *WHO Classification of Tumours of Haematopoietic and Lymphoid Tissues*; Swerdlow, S.H., Campo, E., Harris, N.L., Jaffe, E.S., Pileri, S.A., Stein, H., Thiele, J., Arber, D.A., Hasserjian, R.P., Le Beau, M.M., et al., Eds.; WHO, International Agency for Research on Cancer: Lyon, France, 2017; pp. 156–166.
96. D’Atri, L.P.; Rodríguez, C.S.; Miguel, C.P.; Pozner, R.G.; Ortiz Wilczyński, J.M.; Negrotto, S.; Carrera-Silva, E.A.; Heller, P.G.; Schattner, M. Activation of toll-like receptors 2 and 4 on CD34⁺ cells increases human megakaryo/thrombopoiesis induced by thrombopoietin. *J. Thromb. Haemost.* **2019**, *17*, 2196–2210. [[CrossRef](#)] [[PubMed](#)]
97. Gjertsen, B.T.; Øyan, A.M.; Marzolf, B.; Hovland, R.; Gausdal, G.; Døskeland, S.O.; Dimitrov, K.; Golden, A.; Kalland, K.H.; Hood, L.; et al. Analysis of acute myelogenous leukemia: Preparation of samples for genomic and proteomic analyses. *J. Hematother. Stem Cell Res.* **2002**, *11*, 469–481. [[CrossRef](#)] [[PubMed](#)]
98. Bruserud, Ø.; Gjertsen, B.T.; Foss, B.; Huang, T.S. New strategies in the treatment of acute myelogenous leukemia (AML): In vitro culture of aml cells—The present use in experimental studies and the possible importance for future therapeutic approaches. *Stem Cells* **2001**, *19*, 1–11. [[CrossRef](#)] [[PubMed](#)]

99. Bruserud, Ø.; Hovland, R.; Wergeland, L.; Huang, T.S.; Gjertsen, B.T. Flt3-mediated signaling in human acute myelogenous leukemia (AML) blasts: A functional characterization of Flt3-ligand effects in AML cell populations with and without genetic Flt3 abnormalities. *Haematologica* **2003**, *88*, 416–428. [[PubMed](#)]
100. de Jonge, H.J.M.; Valk, P.J.M.; de Bont, E.S.J.M.; Schuringa, J.J.; Ossenkoppele, G.; Vellenga, E.; Huls, G. Prognostic impact of white blood cell count in intermediate risk acute myeloid leukemia: Relevance of mutated NPM1 and FLT3-ITD. *Haematologica* **2011**, *96*, 1310–1317. [[CrossRef](#)] [[PubMed](#)]
101. Lin, P.; Chen, L.; Luthra, R.; Konoplev, S.N.; Wang, X.M.; Medeiros, L.J. Acute myeloid leukemia harboring t(8;21)(q22;q22): A heterogeneous disease with poor outcome in a subset of patients unrelated to secondary cytogenetic aberrations. *Mod. Pathol.* **2008**, *21*, 1029–1036. [[CrossRef](#)] [[PubMed](#)]
102. Wheatley, K.; Burnett, A.K.; Goldstone, A.H.; Gray, R.G.; Hann, I.M.; Harrison, C.J.; Rees, J.K.H.; Stevens, R.F.; Walker, H. A simple, robust, validated and highly predictive index for the determination of risk-directed therapy in acute myeloid leukaemia derived from the MRC AML 10 trial. *Br. J. Haematol.* **1999**, *107*, 69–79. [[CrossRef](#)] [[PubMed](#)]
103. Feng, S.L.; Zhou, L.; Zhang, X.H.; Tang, B.L.; Zhu, X.Y.; Liu, H.L.; Sun, Z.M.; Zheng, C.C. Impact Of ELN Risk Stratification, Induction Chemotherapy Regimens And Hematopoietic Stem Cell Transplantation On Outcomes In Hyperleukocytic Acute Myeloid Leukemia with Initial White Blood Cell Count More Than $100 \times 10^9/L$. *Cancer Manag. Res.* **2019**, *11*, 9495–9503. [[CrossRef](#)] [[PubMed](#)]
104. How, J.; Sykes, J.; Gupta, V.; Yee, K.W.; Schimmer, A.D.; Schuh, A.C.; Minden, M.D.; Kamel-Reid, S.; Brandwein, J.M. Influence of FLT3-internal tandem duplication allele burden and white blood cell count on the outcome in patients with intermediate-risk karyotype acute myeloid leukemia. *Cancer* **2012**, *118*, 6110–6117. [[CrossRef](#)] [[PubMed](#)]
105. Brenner, A.K.; Bruserud, Ø. Functional Toll-Like Receptors (TLRs) Are Expressed by a Majority of Primary Human Acute Myeloid Leukemia Cells and Inducibility of the TLR Signaling Pathway Is Associated with a More Favorable Phenotype. *Cancers* **2019**, *11*, 973. [[CrossRef](#)] [[PubMed](#)]
106. Borrello, S.; Nicolò, C.; Delogu, G.; Pandolfi, F.; Ria, F. TLR2: A crossroads between infections and autoimmunity? *Int. J. Immunopathol. Pharmacol.* **2011**, *24*, 549–556. [[CrossRef](#)]
107. Erridge, C. Endogenous ligands of TLR2 and TLR4: Agonists or assistants? *J. Leukoc. Biol.* **2010**, *87*, 989–999. [[CrossRef](#)] [[PubMed](#)]
108. Bruserud, Ø.; Reikvam, H.; Brenner, A.K. Toll-like Receptor 4, Osteoblasts and Leukemogenesis; the Lesson from Acute Myeloid Leukemia. *Molecules* **2022**, *27*, 735. [[CrossRef](#)] [[PubMed](#)]
109. Laouedj, M.; Tardif, M.R.; Gil, L.; Raquil, M.A.; Lachhab, A.; Pelletier, M.; Tessier, P.A.; Barabé, F. S100A9 induces differentiation of acute myeloid leukemia cells through TLR4. *Blood* **2017**, *129*, 1980–1990. [[CrossRef](#)] [[PubMed](#)]
110. Kovačić, M.; Mitrović-Ajtić, O.; Beleslin-Čokić, B.; Djikić, D.; Subotički, T.; Diklić, M.; Leković, D.; Gotić, M.; Mossuz, P.; Čokić, V.P. TLR4 and RAGE conversely mediate pro-inflammatory S100A8/9-mediated inhibition of proliferation-linked signaling in myeloproliferative neoplasms. *Cell Oncol.* **2018**, *41*, 541–553. [[CrossRef](#)] [[PubMed](#)]
111. Pang, X.; He, X.; Qiu, Z.; Zhang, H.; Xie, R.; Liu, Z.; Gu, Y.; Zhao, N.; Xiang, Q.; Cui, Y. Targeting integrin pathways: Mechanisms and advances in therapy. *Signal Transduct. Target. Ther.* **2023**, *8*, 1. [[CrossRef](#)]
112. Alasseiri, M.; Ahmed, A.U.; Williams, B.R.G. Mechanisms and consequences of constitutive activation of integrin-linked kinase in acute myeloid leukemia. *Cytokine Growth Factor Rev.* **2018**, *43*, 1–7. [[CrossRef](#)] [[PubMed](#)]
113. Ogana, H.A.; Hurwitz, S.; Wei, N.; Lee, E.; Morris, K.; Parikh, K.; Kim, Y.M. Targeting integrins in drug-resistant acute myeloid leukaemia. *Br. J. Pharmacol.* **2024**, *181*, 295–316. [[CrossRef](#)]
114. Kim, H.N.; Ruan, Y.; Ogana, H.; Kim, Y.M. Cadherins, Selectins, and Integrins in CAM- DR in Leukemia. *Front. Oncol.* **2020**, *10*, 592733. [[CrossRef](#)] [[PubMed](#)]
115. Mosaddeghzadeh, N.; Ahmadian, M.R. The RHO Family GTPases: Mechanisms of Regulation and Signaling. *Cells* **2021**, *10*, 1831. [[CrossRef](#)] [[PubMed](#)]
116. D’Amato, L.; Dell’Aversana, C.; Conte, M.; Ciotta, A.; Scisciola, L.; Carissimo, A.; Nebbioso, A.; Altucci, L. ARHGEF3 controls HDACi-induced differentiation via RhoA-dependent pathways in acute myeloid leukemias. *Epigenetics* **2015**, *10*, 6–18. [[CrossRef](#)] [[PubMed](#)]
117. Reuther, G.W.; Lambert, Q.T.; Booden, M.A.; Wennerberg, K.; Becknell, B.; Marcucci, G.; Sondek, J.; Caligiuri, M.A.; Der, C.J. Leukemia-associated Rho guanine nucleotide exchange factor, a Dbl family protein found mutated in leukemia, causes transformation by activation of RhoA. *J. Biol. Chem.* **2001**, *276*, 27145–27151. [[CrossRef](#)] [[PubMed](#)]
118. Lee, S.H.; Chiu, Y.C.; Li, Y.H.; Lin, C.C.; Hou, H.A.; Chou, W.C.; Tien, H.F. High expression of *dedicator of cytokinesis (DOCK1)* confers poor prognosis in acute myeloid leukemia. *Oncotarget* **2017**, *8*, 72250–72259. [[CrossRef](#)]
119. Yang, S.H.; Liu, W.; Peng, J.; Xu, Y.J.; Liu, Y.F.; Li, Y.; Peng, M.Y.; Ou-Yang, Z.; Chen, C.; Liu, E.Y. High Expression of RhoBTB3 Predicts Favorable Chemotherapy Outcomes in non-M3 Acute Myeloid Leukemia. *J. Cancer* **2021**, *12*, 4229–4239. [[CrossRef](#)] [[PubMed](#)]
120. Liang, X.; Xia, R. Kinesin family member 2A acts as a potential prognostic marker and treatment target via interaction with PI3K/AKT and RhoA/ROCK pathways in acute myeloid leukemia. *Oncol. Rep.* **2022**, *47*, 18. [[CrossRef](#)] [[PubMed](#)]

121. Brenner, A.K.; Bruserud, Ø. S100 Proteins in Acute Myeloid Leukemia. *Neoplasia* **2018**, *20*, 1175–1186. [[CrossRef](#)] [[PubMed](#)]
122. Mondet, J.; Chevalier, S.; Mossuz, P. Pathogenic Roles of S100A8 and S100A9 Proteins in Acute Myeloid and Lymphoid Leukemia: Clinical and Therapeutic Impacts. *Molecules* **2021**, *26*, 1323. [[CrossRef](#)]
123. Zhang, L.; Zhu, T.; Miao, H.; Liang, B. The Calcium Binding Protein S100A11 and Its Roles in Diseases. *Front. Cell Dev. Biol.* **2021**, *9*, 693262. [[CrossRef](#)] [[PubMed](#)]
124. Mosesson, M.W. Fibrinogen and fibrin structure and functions. *J. Thromb. Haemost.* **2005**, *3*, 1894–1904. [[CrossRef](#)]
125. Redman, C.M.; Xia, H. Fibrinogen biosynthesis. Assembly, intracellular degradation, and association with lipid synthesis and secretion. *Ann. N. Y. Acad. Sci.* **2001**, *936*, 480–495. [[CrossRef](#)]
126. Luyendyk, J.P.; Schoenecker, J.G.; Flick, M.J. The multifaceted role of fibrinogen in tissue injury and inflammation. *Blood* **2019**, *133*, 511–520. [[CrossRef](#)]
127. Orino, K.; Yamamoto, S.; Watanabe, K. Fibrinogen as a ferritin-binding protein in horse plasma. *J. Vet. Med. Sci.* **1993**, *55*, 785–787. [[CrossRef](#)] [[PubMed](#)]
128. Lebon, D.; Vergez, F.; Bertoli, S.; Harrivel, V.; De Botton, S.; Micol, J.B.; Marolleau, J.P.; Récher, C. Hyperferritinemia at diagnosis predicts relapse and overall survival in younger AML patients with intermediate-risk cytogenetics. *Leuk. Res.* **2015**, *39*, 818–821. [[CrossRef](#)]
129. Zhou, C.; Yang, L.; Zhao, K.; Jiang, L. ITGAM sustains MAPK signaling and serves as an adverse prognostic factor and therapeutic target in acute myeloid leukemia. *Transl. Cancer Res.* **2024**, *13*, 3062–3074. [[CrossRef](#)] [[PubMed](#)]
130. Gong, R.; Li, H.; Liu, Y.; Wang, Y.; Ge, L.; Shi, L.; Wu, G.; Lyu, J.; Gu, H.; He, L. Gab2 promotes acute myeloid leukemia growth and migration through the SHP2-Erk-CREB signaling pathway. *J. Leukoc. Biol.* **2022**, *12*, 669–677. [[CrossRef](#)]
131. Lin, L.; Que, Y.; Lu, P.; Li, H.; Xiao, M.; Zhu, X.; Li, D. Chidamide Inhibits Acute Myeloid Leukemia Cell Proliferation by lncRNA VPS9D1-AS1 Downregulation via MEK/ERK Signaling Pathway. *Front. Pharmacol.* **2020**, *11*, 569651. [[CrossRef](#)] [[PubMed](#)]
132. Kumar, S.; Farah, I.O.; Tchounwou, P.B. Trisenox induces cytotoxicity through phosphorylation of mitogen-activated protein kinase molecules in acute leukemia cells. *J. Biochem. Mol. Toxicol.* **2018**, *32*, e22207. [[CrossRef](#)]
133. Zabkiewicz, J.; Lazenby, M.; Edwards, G.; Bygrave, C.A.; Omidvar, N.; Zhuang, L.; Knapper, S.; Guy, C.; Hills, R.K.; Burnett, A.K.; et al. Combination of a mitogen-activated protein kinase inhibitor with the tyrosine kinase inhibitor pacritinib combats cell adhesion-based residual disease and prevents re-expansion of FLT3-ITD acute myeloid leukaemia. *Br. J. Haematol.* **2020**, *191*, 231–242. [[CrossRef](#)] [[PubMed](#)]
134. Zhang, W.; Konopleva, M.; Burks, J.K.; Dywer, K.C.; Schober, W.D.; Yang, J.Y.; McQueen, T.J.; Hung, M.C.; Andreeff, M. Blockade of mitogen-activated protein kinase/extracellular signal-regulated kinase and murine double minute synergistically induces Apoptosis in acute myeloid leukemia via BH3-only proteins Puma and Bim. *Cancer Res.* **2010**, *70*, 2424–2434. [[CrossRef](#)] [[PubMed](#)]
135. Kojima, K.; Konopleva, M.; Samudio, I.J.; Ruvolo, V.; Andreeff, M. Mitogen-activated protein kinase inhibition enhances nuclear proapoptotic function of p53 in acute myelogenous leukemia cells. *Cancer Res.* **2007**, *67*, 3210–3219. [[CrossRef](#)] [[PubMed](#)]
136. Borthakur, G.; Popplewell, L.; Boyiadzis, M.; Foran, J.; Platzbecker, U.; Vey, N.; Walter, R.B.; Olin, R.; Raza, A.; Giagounidis, A.; et al. Activity of the oral mitogen-activated protein kinase kinase inhibitor trametinib in RAS-mutant relapsed or refractory myeloid malignancies. *Cancer* **2016**, *122*, 1871–1879. [[CrossRef](#)]
137. Stewart, H.J.S.; Chaudry, S.; Crichlow, A.; Luiling Feilding, F.; Chevassut, T.J.T. BET Inhibition Suppresses S100A8 and S100A9 Expression in Acute Myeloid Leukemia Cells and Synergises with Daunorubicin in Causing Cell Death. *Bone Marrow Res.* **2018**, *2018*, 5742954. [[CrossRef](#)]
138. Böttcher, M.; Panagiotidis, K.; Bruns, H.; Stumpf, M.; Völkl, S.; Geyh, S.; Dietel, B.; Schroeder, T.; Mackensen, A.; Mougiakakos, D. Bone marrow stroma cells promote induction of a chemoresistant and prognostic unfavorable S100A8/A9high AML cell subset. *Blood Adv.* **2022**, *6*, 5685–5697. [[CrossRef](#)] [[PubMed](#)]
139. Ramos, D.F.V.; Mancuso, R.I.; Contieri, B.; Duarte, A.; Paiva, L.; de Melo Carrilho, J.; Saad, S.T.O.; Lazarini, M. Rac GTPases in acute myeloid leukemia cells: Expression profile and biological effects of pharmacological inhibition. *Toxicol. Appl. Pharmacol.* **2022**, *442*, 115990. [[CrossRef](#)]
140. Wen, X.; Li, P.; Ma, Y.; Wang, D.; Jia, R.; Xia, Y.; Li, W.; Li, Y.; Li, G.; Sun, T.; et al. RHOF activation of AKT/ β -catenin signaling pathway drives acute myeloid leukemia progression and chemotherapy resistance. *iScience* **2024**, *27*, 110221. [[CrossRef](#)] [[PubMed](#)]
141. Rahmati, A.; Goudarzi, S.; Sheikhi, M.; Siyadat, P.; Ferns, G.A.; Ayatollahi, H. The Emerging Roles of Aldehyde Dehydrogenase in Acute Myeloid Leukemia and Its Therapeutic Potential. *Anticancer Agents Med. Chem.* **2023**, *23*, 246–255. [[PubMed](#)]
142. Dancik, G.M.; Voutsas, I.F.; Vlahopoulos, S. Aldehyde Dehydrogenase Enzyme Functions in Acute Leukemia Stem Cells. *Front. Biosci. (Sch. Ed.)* **2022**, *14*, 8. [[CrossRef](#)]
143. Dancik, G.M.; Varisli, L.; Vlahopoulos, S.A. The Molecular Context of Oxidant Stress Response in Cancer Establishes ALDH1A1 as a Critical Target: What This Means for Acute Myeloid Leukemia. *Int. J. Mol. Sci.* **2023**, *24*, 9372. [[CrossRef](#)]
144. Dancik, G.M.; Voutsas, I.F.; Vlahopoulos, S. Lower RNA expression of ALDH1A1 distinguishes the favorable risk group in acute myeloid leukemia. *Mol. Biol. Rep.* **2022**, *49*, 3321–3331. [[CrossRef](#)] [[PubMed](#)]

145. Jiang, N.; Zhang, X.; Chen, Q.; Kantawong, F.; Wan, S.; Liu, J.; Li, H.; Zhou, J.; Lu, B.; Wu, J. Identification of a Mitochondria-Related Gene Signature to Predict the Prognosis in AML. *Front. Oncol.* **2022**, *12*, 823831. [[CrossRef](#)]
146. Tong, X.; Zhou, F. Integrated bioinformatic analysis of mitochondrial metabolism-related genes in acute myeloid leukemia. *Front. Immunol.* **2023**, *14*, 1120670. [[CrossRef](#)]
147. Hoyle, C.F.; Gray, R.G.; Wheatley, K.; Swirsky, D.; de Bastos, M.; Sherrington, P.; Rees, J.K.; Hayhoe, F.G. Prognostic importance of Sudan Black positivity: A study of bone marrow slides from 1,386 patients with de novo acute myeloid leukaemia. *Br. J. Haematol.* **1991**, *79*, 398–407. [[CrossRef](#)]
148. Kanda, Y.; Hamaki, T.; Yamamoto, R.; Chizuka, A.; Suguro, M.; Matsuyama, T.; Takezako, N.; Miwa, A.; Kami, M.; Hirai, H.; et al. The clinical significance of CD34 expression in response to therapy of patients with acute myeloid leukemia: An overview of 2483 patients from 22 studies. *Cancer* **2000**, *88*, 2529–2533. [[CrossRef](#)]
149. Dang, H.; Chen, Y.; Kamel-Reid, S.; Brandwein, J.; Chang, H. CD34 expression predicts an adverse outcome in patients with NPM1-positive acute myeloid leukemia. *Hum. Pathol.* **2013**, *44*, 2038–2046. [[CrossRef](#)]
150. Zhu, H.H.; Liu, Y.R.; Jiang, H.; Lu, J.; Qin, Y.Z.; Jiang, Q.; Bao, L.; Ruan, G.R.; Jiang, B.; Huang, X. CD34 expression on bone marrow blasts is a novel predictor of poor prognosis independent of FLT3-ITD in acute myeloid leukemia with the NPM1-mutation. *Leuk. Res.* **2013**, *37*, 624–630. [[CrossRef](#)] [[PubMed](#)]
151. Short, N.J.; Zhou, S.; Fu, C.; Berry, D.A.; Walter, R.B.; Freeman, S.D.; Hourigan, C.S.; Huang, X.; Nogueras Gonzalez, G.; Hwang, H.; et al. Association of Measurable Residual Disease with Survival Outcomes in Patients with Acute Myeloid Leukemia: A Systematic Review and Meta-analysis. *JAMA Oncol.* **2020**, *6*, 1890–1899. [[CrossRef](#)] [[PubMed](#)]
152. Chea, M.; Rigolot, L.; Canali, A.; Vergez, F. Minimal Residual Disease in Acute Myeloid Leukemia: Old and New Concepts. *Int. J. Mol. Sci.* **2024**, *25*, 2150. [[CrossRef](#)]
153. Schwind, S.; Jentzsch, M.; Bach, E.; Stasik, S.; Thiede, C.; Platzbecker, U. Use of Minimal Residual Disease in Acute Myeloid Leukemia Therapy. *Curr. Treat. Options Oncol.* **2020**, *21*, 8. [[CrossRef](#)] [[PubMed](#)]
154. Zeijlemaker, W.; Grob, T.; Meijer, R.; Hanekamp, D.; Kelder, A.; Carbaat-Ham, J.C.; Oussoren-Brockhoff, Y.J.M.; Snel, A.N.; Veldhuizen, D.; Scholten, W.J.; et al. CD34⁺CD38⁻ leukemic stem cell frequency to predict outcome in acute myeloid leukemia. *Leukemia* **2019**, *33*, 1102–1112. [[CrossRef](#)]
155. Bruserud, Ø.; Liseth, K.; Stamnesfet, S.; Cacic, D.L.; Melve, G.; Kristoffersen, E.; Hervig, T.; Reikvam, H. Hyperleukocytosis and leukocytapheresis in acute leukaemias: Experience from a single centre and review of the literature of leukocytapheresis in acute myeloid leukaemia. *Transfus. Med.* **2013**, *23*, 397–406. [[CrossRef](#)] [[PubMed](#)]
156. Bewersdorf, J.P.; Zeidan, A.M. Hyperleukocytosis and Leukostasis in Acute Myeloid Leukemia: Can a Better Understanding of the Underlying Molecular Pathophysiology Lead to Novel Treatments? *Cells* **2020**, *9*, 2310. [[CrossRef](#)] [[PubMed](#)]
157. Brenner, A.K.; Tvedt, T.H.; Nepstad, I.; Rye, K.P.; Hagen, K.M.; Reikvam, H.; Bruserud, Ø. Patients with acute myeloid leukemia can be subclassified based on the constitutive cytokine release of the leukemic cells; the possible clinical relevance and the importance of cellular iron metabolism. *Expert Opin. Ther. Targets* **2017**, *21*, 357–369. [[CrossRef](#)] [[PubMed](#)]
158. Forgrave, L.M.; Wang, M.; Yang, D.; DeMarco, M.L. Proteoforms and their expanding role in laboratory medicine. *Pract. Lab. Med.* **2021**, *28*, e00260. [[CrossRef](#)] [[PubMed](#)]
159. Smith, L.M.; Agar, J.N.; Chamot-Rooke, J.; Danis, P.O.; Ge, Y.; Loo, J.A.; Paša-Tolić, L.; Tsybin, Y.O.; Kelleher, N.L.; Consortium for Top-Down Proteomics. The Human Proteoform Project: Defining the human proteome. *Sci. Adv.* **2021**, *7*, eabk0734. [[CrossRef](#)]
160. Coorssen, J.R.; Padula, M.P. Proteomics-The State of the Field: The Definition and Analysis of Proteomes Should Be Based in Reality, Not Convenience. *Proteomes* **2024**, *12*, 14. [[CrossRef](#)]
161. Shvedunova, M.; Akhtar, A. Modulation of cellular processes by histone and non-histone protein acetylation. *Nat. Rev. Mol. Cell Biol.* **2022**, *23*, 329–349. [[CrossRef](#)] [[PubMed](#)]
162. Narita, T.; Weinert, B.T.; Choudhary, C. Functions and mechanisms of non-histone protein acetylation. *Nat. Rev. Mol. Cell Biol.* **2019**, *20*, 156–174. [[CrossRef](#)]
163. Wang, S.; Osgood, A.O.; Chatterjee, A. Uncovering post-translational modification-associated protein-protein interactions. *Curr. Opin. Struct. Biol.* **2022**, *74*, 102352. [[CrossRef](#)] [[PubMed](#)]
164. Han, Z.J.; Feng, Y.H.; Gu, B.H.; Li, Y.M.; Chen, H. The post-translational modification, SUMOylation, and cancer. *Int. J. Oncol.* **2018**, *52*, 1081–1094. [[CrossRef](#)]
165. Wang, Y.; Yan, D.; Liu, J.; Tang, D.; Chen, X. Protein modification and degradation in ferroptosis. *Redox Biol.* **2024**, *75*, 103259. [[CrossRef](#)] [[PubMed](#)]

Disclaimer/Publisher's Note: The statements, opinions and data contained in all publications are solely those of the individual author(s) and contributor(s) and not of MDPI and/or the editor(s). MDPI and/or the editor(s) disclaim responsibility for any injury to people or property resulting from any ideas, methods, instructions or products referred to in the content.